Summer 2014

Performance analysis of zero forcing and minimum mean square error equalizers on multiple input multiple output system on a spinning vehicle

Aditya Kulkarni

Department:

PERFORMANCE ANALYSIS OF ZERO FORCING AND MINIMUM MEAN SQUARE ERROR EQUALIZERS ON MULTIPLE INPUT MULTIPLE OUTPUT SYSTEM ON A SPINNING VEHICLE

by

ADITYA KULKARNI

A THESIS

Presented to the Faculty of the Graduate School of the

MISSOURI UNIVERSITY OF SCIENCE AND TECHNOLOGY

In Partial Fulfillment of the Requirements for the Degree

MASTER OF SCIENCE IN ELECTRICAL ENGINEERING

2014

Approved by

Dr. Kurt Kosbar, Advisor
Dr. Maciej Zawodniok
Dr. Steve Grant

ABSTRACT

Channel equalizers based on minimum mean square error (MMSE) and zero forcing (ZF) criteria have been formulated for a general scalable multiple input multiple output (MIMO) system and implemented for a 2x2 MIMO system with spatial multiplexing (SM) for Rayleigh channel associated with additive white Gaussian noise. A model to emulate transmitters and receivers on a spinning vehicle has been developed. A transceiver based on the BLAST architecture is developed in this work. A mathematical framework to explain the behavior of the ZF and MMSE equalizers is formulated. The performance of the equalizers has been validated for a case with one of the communication entities being a spinning aero-vehicle. Performance analysis with respect to variation of angular separation between the antennas and relative antenna gain for each case is presented. Based on the simulation results a setup with optimal design parameters for placement of antennas, choice of the equalizers and transmit power is proposed.

ACKNOWLEDGMENTS

I would like to take this opportunity to express my heartfelt gratitude to a number of people who have helped me during the course of my Masters. First of all I would like to thank my advisor, Dr. Kurt Kosbar for all his guidance and providing me the opportunity to work in the Telemetry Learning Center at Missouri S&T.

I am grateful to my advising committee Dr. Maciej Zawodniok and Dr. Steve Grant for their valuable suggestions. I also express my gratitude to the staff of the Electrical Engineering Department and the Office of Graduate Studies at Missouri S&T for their support.

Finally, I would like to express my gratitude to my family and friends who have been a constant source of support and motivation.

TABLE OF CONTENTS

LIST OF ILLUSTRATIONS

Page

1. INTRODUCTION

Reliable and high speed wireless communication systems have ubiquitous demand. One of the breakthroughs in the area of wireless communications is the development of Multiple Input Multiple Output (MIMO) systems that multiple antennas at transmitter and receiver. Many techniques have been developed to upgrade the performance of MIMO systems in variety of applications [1-10].

Aerospace telemetry offers an interesting application for MIMO systems. Aero nautical vehicles can follow a complex pattern of motion. Such systems are also often associated with challenging conditions such as low bandwidth and Signal to Noise Ratio (SNR). In this case a Single Input Single Output (SISO) system, that is a communication system with one transmitter and one receiver antenna, may suffer a severe degradation of performance because of a large fraction of the transmit power directed away from the receiver. MIMO systems can effectively address these issues by reducing the probability of loss of link, improve the error rate, and generally increase performance.

In this thesis a MIMO system with one of the entities being a spinning aero-vehicle is considered. Figure 1.1 illustrates the geometry of the problem. The antennas at both ends of the link are placed several wavelengths apart so that the individual channel paths are uncorrelated [15,16].

Figure 1.1 shows a rotating aero-vehicle and a base station that form a 2x2 MIMO system. θ represents the angle between an imaginary line drawn in the direction pointed by one of the antennas on the spinning vehicle and an imaginary line drawn between the antennas of the base station. This angle is measured by considering a vertical cut. The aero-vehicle is shown to be spinning at an angular frequency of ω radians per seconds. The antennas are placed laterally on the cylindrical aero-vehicle. The angular separation between the antennas is represented by ϕ radians. The distance between the antennas at the base station is represented by r.

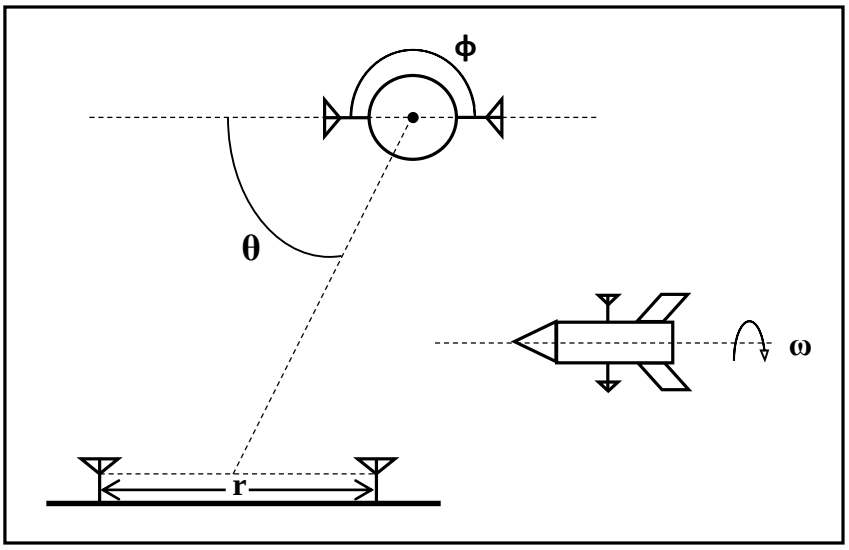

Figure 1.1 Problem Geometry

The system involves air-to-ground and ground-to-air communication. In this case the communication link is associated with significant multipath in a rich scattering environment. Bell Laboratories Layered Space Time (BLAST) architecture [17, 21] has been developed to exploit such conditions and achieve enhanced performance of a MIMO setup. In a simplified sense it involves spatial multiplexing at the transmitter, that is simultaneous transmission of multiple data streams in the same frequency band and the detection process primarily includes an equalizer to abate inter-symbol interference (ISI) and inter-channel interference.

A transceiver based on the BLAST architecture is developed in this work. A spatial multiplexing technique is implemented at the transmitter, in other words the transmitter sends digitally modulated binary bits as parallel data streams. A Rayleigh flat fading channel corrupted by additive white Gaussian noise (AWGN) is used to emulate the channel behavior. The spin of the vehicle gives a predictable component to the channel. This is mathematically formulated using a sine-wave model.

Inter-symbol Interference severely affects the performance of a receiver in a MIMO system. One of the effective means to abate ISI is by a filtering technique called

equalization. In this work two equalizers for a general N_T by N_R MIMO system (N_T represents the number of transmitters and N_R represents the number of receivers) are formulated based on minimum mean square error (MMSE) and zero forcing (ZF) criteria. The receiver is assumed to have the perfect knowledge of the channel state and the weights of the equalizing filters are dynamically computed.

A mathematical framework to indicate the output SNR of the ZF and MMSE equalizers is formulated. This serves to be a key indicator of performance of equalizers in static and dynamic scenarios. A MIMO model with spatial multiplexing and equalization in accordance with the BLAST architecture is developed. The spin of the vehicle is simulated with the sine wave model makes the channel coefficients to have a periodic component. The model is applied to a system that has one of the communication entities, that is either the transmitter or receiver mounted on a spinning vehicle.

Firstly, the system is verified for correctness by comparing it to a scenario where the transmitter and receiver are stationary. In this case the performance of the MMSE equalizer is seen to be nearly 3dB better than ZF equalizer. The performance of the receiver in case of the spinning vehicle is studied in two scenarios. In the first case, the spinning vehicle transmits data and the stationary base station is the receiver. In this case ZF equalizer closely follows the performance of an MMSE equalizer. In the second case with the spinning vehicle is the receiver and the stationary base station is the transmitter, the MMSE equalizer is seen to have a superior performance.

The effect of beam-width of antenna on the performance of the system is studied. It is found that for highly directive antenna, the gain in performance with increase in SNR is negligible. The spatial configuration of the antennas on the spinning vehicles is seen to affect the performance. Increased efficiency in performance is achieved with the antennas mounted on the spinning vehicle are separated by π radians. Based on these observation a few design optimizations to increase efficiency and reduce complexity are proposed.

2. BACKGROUND INFORMATION

2.1. WIRELESS COMMUNICATION

Figure 2.1 presents a basic communication block diagram. Transmitter, channel and receiver constitute a wireless communication system. Transmitter sends the information using electromagnetic waves. The propagation medium of the electromagnetic waves is the channel. The receiver extracts information from the transmitted signal.

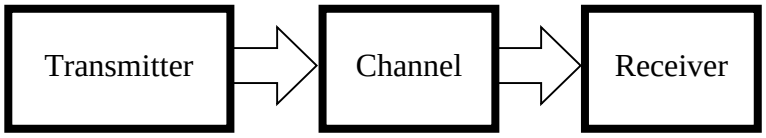

Figure 2.1 Basic Communication System

A block diagram to indicate the necessary functional blocks of a digital communication system is presented in Figure 2.2. Data source generates binary data stream. Typically analog signals such as audio or video are quantized and converted into digital format.

Efficient representation of such a data to achieve high data rates and avoid redundancy is important to effectively communicate through a noisy channel. On the basis of information theory several techniques have been developed to achieve this goal. A device that implements such techniques to offer one-to-one mapping of a digital data bits to a new reduced format is called a source encoder.

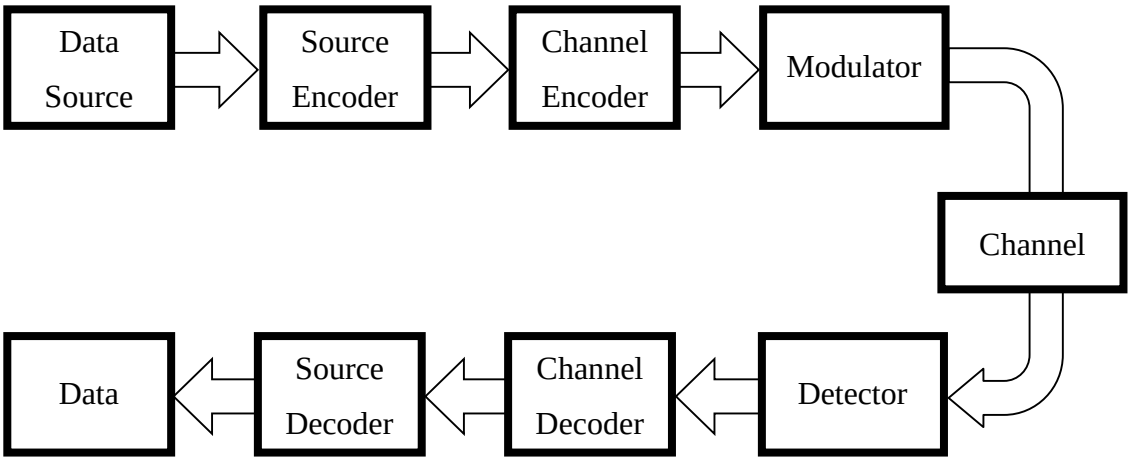

Figure 2.2 Block Diagram of a Digital Communication System

The presence of noise in the channel corrupts the transmitted signal. In many applications highly reliable communication is critical. Reliability is achieved by introducing controlled redundancy in a pre-designed mechanism. A channel encoder implements this technique.

Modulation is a process by which some characteristic of a carrier wave (typically a sinusoid) such as amplitude, phase or frequency is varied in accordance with a modulating wave to increase efficiency of transmission. A modulator implements baseband modulation or pulse-code modulation and band-pass modulation or RF modulation that forms two stages of the digital modulation technique.

The receiver design is symmetric to the transmitter. Each functional block of a receiver is an inverse of its counterpart in the transmitter [18].

2.2. MULTIPATH

Due to reflection, diffraction and refraction of the transmitted signal, multiple copies of the transmitted signal are received with different amplitude and delay. This phenomenon is called multipath effect.

Fading channels are model the corruption of the signal during multipath propagation. Figure 2.3 illustrates a narrowband or a flat fading channel where the delay between the multipath components is less than the symbol interval (T_s). Figure 2.4 illustrates a wideband or frequency selective fading channel where the multipath components have a delay that is greater than the symbol interval. Inter-symbol Interference (ISI) and Inter-carrier Interference (ICI) are consequences of multipath effect [28].

Figure 2.3 Narrowband Channel

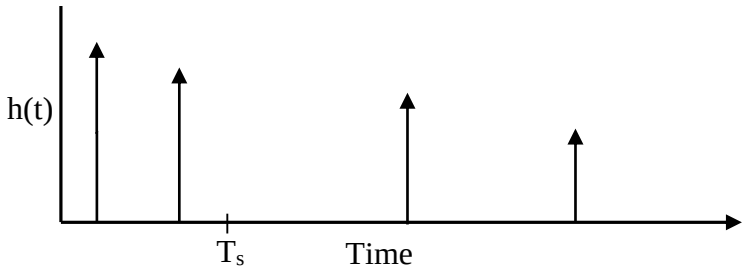

Figure 2.4 Wideband Channel

2.3. BPSK MODULATION

BPSK is a common digital modulation technique that maps binary data, 0 and 1 to $\sqrt{E_b}$ or -$\sqrt{E_b}$, respectively, where E_b is the average energy per bit. The input binary sequence is modeled as an independent and identically distributed random variable that is probability of 0 and 1 is equal to 50%. The baseband modulation can be perceived as a summation of shifted pulse waveforms. The piecewise equation for a pulse waveform is given in equation 1.

$$p(t) = \begin{cases} 1, & 0 \le t \le T_b \\ 0, & otherwise \end{cases} \quad (1)$$

Here T_b refers to a bit interval.

The baseband modulated wave $s_b(t)$ is obtained as defined in equation 2.

$$s_b(t) = \sum_{k=1}^{N} (2d_k - 1)p(t - kT_b) \quad (2)$$

Here d_k is the transmitted binary bit, '0' or '1' at the k^{th} symbol time slot (STS) and N is the total number of bits in the transmit sequence.

Radio Frequency (RF) refers to frequency of radio waves that are widely used in wireless communication application. It varies between vary between 3Khz to 300 Ghz [29]. In the passband the RF carrier wave with a frequency denoted by f_c is modulated by changing the phase by π and 0 for the input binary bit '0' and '1', respectively, for each bit interval T_b. The passband modulated waveform, $s_p(t)$ is represented in equation 3.

$$s_p(t) = c(t) = \sqrt{\frac{2E_b}{T_b}}.\cos(2\pi f_c t + (d_k - 1)\pi) \tag{3}$$

From equation 3, we see that the signal-space for BPSK modulation can be represented by the basis functions $\phi_1(t) = \sqrt{\frac{2}{T_b}}\cos(2\pi f_c t)$ and $\phi_2(t) = \sqrt{\frac{2}{T_b}}\sin(2\pi f_c t)$ for $0 \leq t \leq T_b$. Figure 2.5 represents the BPSK signal constellation.

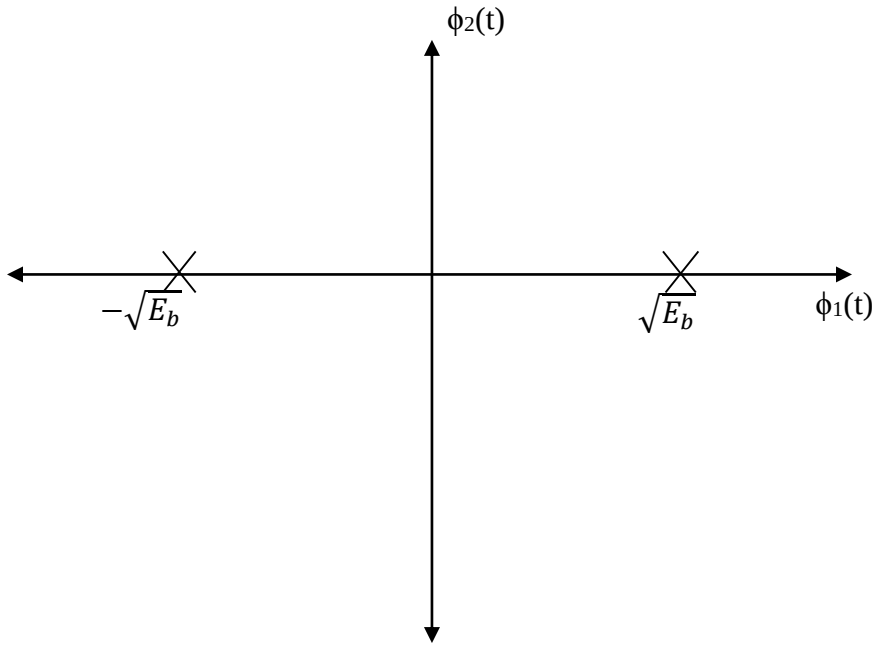

Figure 2.5 BPSK Constellation Plot

Figure 2.6 depicts up-conversion of $s_{ib}(t)$ and $s_{qb}(t)$ to $s_p(t)$ followed by down-conversion of $s_p(t)$ to $s_{ib}(t)$ and $s_{qb}(t)$. $s_{ib}(t)$ and $s_{qb}(t)$ refer to the in-phase and quadrature phase components of the baseband modulated signal and $s_p(t)$ is the passband modulated signal. For BPSK modulation the quadrature component goes to zero [19, 20].

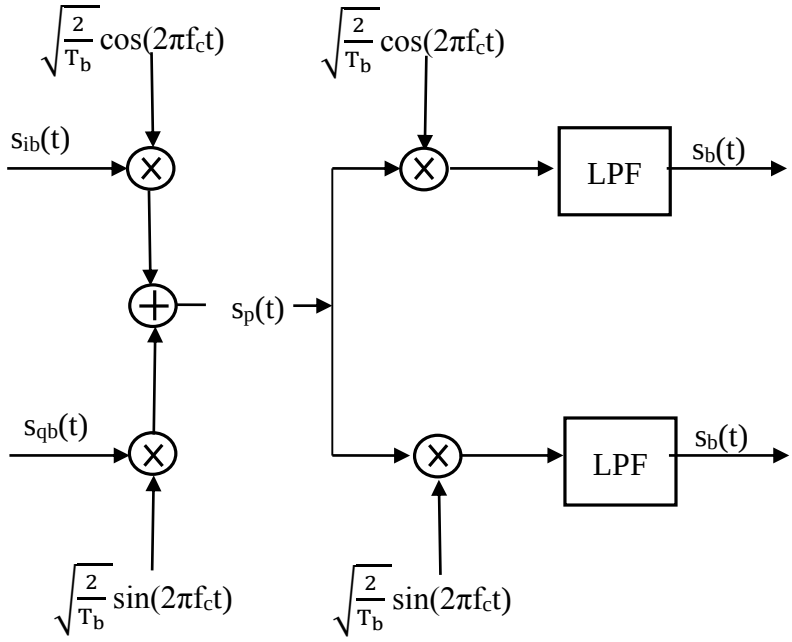

Figure 2.6 Up-conversion and Down-conversion in Digital Modulation

2.4. RAYLEIGH CHANNEL MODEL

The multipath propagation of MIMO system along with scattering can be modeled using a Rayleigh fading channel. When the number of multipath components is sufficiently large, based on central limit theorem the propagation can be modeled as a radial component of two independent Gaussian random distributions. It is a statistical model that assumes uniform scattering in all directions with no Line Of Sight (LOS) component between the transmitter and receiver. The pdf of such a statistical model follows a Rayleigh distribution as seen in equation 4.

$$p(u) = \frac{1}{\sqrt{2\pi}} e^{-\frac{u^2}{2}} \tag{4}$$

2.5. MIMO SYSTEM MODEL

Consider a general N_T by N_R MIMO system with N_T transmit antennas and N_R receive antennas. There will be N_T by N_R uncorrelated paths between the transmitters and receivers. The complex channel gains between i^{th} receiver and j^{th} transmitter at a k^{th} STS is represented as $h_{ij,k}$ given by equation 5 where α_{ij} are the amplitude gain and β_{ij} are the phase shift along these paths. The channel coefficients follow a Rayleigh distribution as given by equation 4. The block diagram for baseband transmission to baseband reception is presented in Figure 2.7.

$$h_{ijk} = \alpha_{ijk} e^{\beta_{ijk}} \tag{5}$$

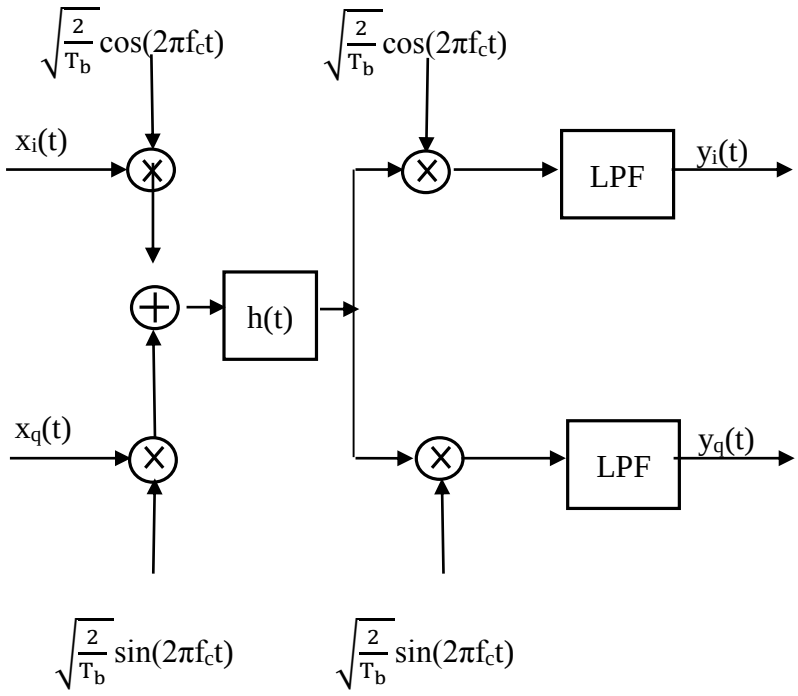

Figure 2.7 Block Diagram for Baseband Transmission to Baseband Reception

Here $x_i(t)$ and $x_q(t)$ are the in-phase and quadrature components of the baseband transmit signal and $y_i(t)$ and $y_q(t)$ are the baseband received signals. The linear model for the system is presented in equation 6 and equation 7. A 2x2 MIMO system is presented in Figure 2.8.

$$\begin{bmatrix} y_{1,k} \\ y_{2,k} \end{bmatrix} = \begin{bmatrix} h_{11,k} & h_{12,k} \\ h_{21,k} & h_{22,k} \end{bmatrix} \begin{bmatrix} x_{1,k} \\ x_{2,k} \end{bmatrix} + \begin{bmatrix} n_{1,k} \\ n_{2,k} \end{bmatrix} \tag{6}$$

$$Y = HX + N \tag{7}$$

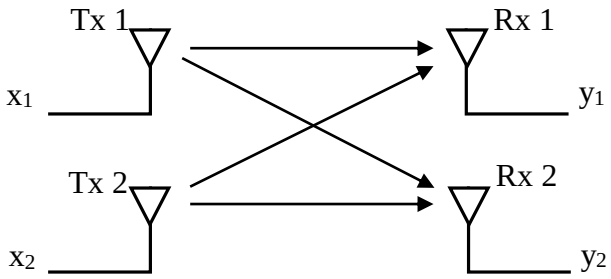

Figure 2.8 A 2x2 MIMO System

X is a set of transmit signal vectors in the signal space defined by a set of basis functions. Y is the corresponding set of received signal vectors.

Noise at the receiver is modeled by an N_R X 1 column vector whose elements are zero-mean, i.i.d. complex Gaussian random variables with identical variances (power) σ^2 [14].

2.6. SPATIAL MULTIPLEXING

MIMO systems provide an additional spatial dimension component that offers a degree-of-freedom-gain. Several techniques have been developed to exploit this fact to achieve gain and efficiency in performance. Some of the popular techniques include transmit diversity, receive diversity, and spatial multiplexing.

In the spatial multiplexing technique, the data is transmitted in independent parallel streams. In a rich scattering channel condition with N_T transmit and N_R receive antennas ($N_R \geq N_T$) this technique provides a linear gain in capacity by a factor of N_T without any increase in transmit power or channel bandwidth. Spatial multiplexing is of

two types, open-loop spatial multiplexing and closed-loop spatial multiplexing. In open-loop spatial multiplexing the transmitter has no channel state information (CSI) where as a closed loop spatial multiplexing scheme the transmitter utilizes the CSI to decrease the correlation between the parallel data streams. Bell Laboratories Space-Time (BLAST) and Selective Per antenna rate control are some models that are apply spatial multiplexing technique [21, 22, 23-27, 19].

2.7. EQUALIZATION

The effect of Inter Symbol Interference (ISI) in multipath time –varying dispersive channel is more severe than noise associated with the system. One method to abate this ISI is by implementing equalization or channel inversion at the receiver. Effectively the equalizers are used to decouple the multiple sub-streams in the received sequence. The process of equalization involves realization of a filter w such that $W(z)$ is approximately equal to $H^{-1}(z)$. In this work a zero forcing equalizer is formulated based on a minimum error criterion and a MMSE equalizer based on minimum mean square error criterion. A generalized expression for these equalizers that can be used for any N_T by N_R MIMO system is presented [13].

2.7.1. Zero Forcing Equalizer. A Zero Forcing equalizer is formulated to render the least square estimate of the transmit signal vector. It is shown that, the Zero Forcing equalizer is the pseudo-inverse of the channel matrix. Hence, the zero forcing equalizer is purely a function of the channel state or the channel matrix [12].

$$\min(|\mathrm{Y} - \mathrm{HX}|) \tag{8}$$

$$\widehat{\mathrm{X}} = (\mathrm{H}\tilde{}\mathrm{H})^{-1}\mathrm{H}\tilde{}\mathrm{Y} \tag{9}$$

where $(.)\tilde{}$ is the hermitian operator that produces the complex conjugate of a matrix.

$$W_{zf} = (H^{\sim}H)^{-1}H^{\sim} \tag{10}$$

With ZF equalization we N_T independent data streams are obtained. The output SNR of n^{th} sub-stream (μ_n) derived below.

$$\hat{X} = X + (H^{\sim}H)^{-1}H^{\sim}N \tag{11}$$

$$\gamma_{zf} = \frac{E(XX^{\sim})}{E((H^{\sim}H)^{-1}H^{\sim}N((H^{\sim}H)^{-1}H^{\sim}N)^{\sim})} \tag{12}$$

where, E(.) represents the expectation function.

$$\gamma_{zf} = \frac{E(XX^{\sim})}{(H^{\sim}H)^{-1}} \tag{13}$$

$$\gamma_{zf} = \frac{\begin{pmatrix} \mu_1 & 0 \\ 0 & \mu_2 \end{pmatrix}}{(H^{\sim}H)^{-1}} \tag{14}$$

$$\gamma_{zf,n} = \frac{\mu_n}{((H^{\sim}H)^{-1})_{nn}}, 1 \leq n \leq N_T \tag{15}$$

2.7.2. Minimum Mean Square Error Equalizer. The Zero Forcing equalizer neglects the effect of noise. A more robust equalizer is proposed based on the Minimum Mean Square Error (MMSE) criterion. The equalizer, $\mathbf{W_{MMSE}}$ renders an estimate of the transmit signal vector such that the mean square error between them is minimum. In this section a brief derivation of the MMSE equalizer is presented. The MMSE criterion is formulated as shown in equation 16 [12].

$$min[E\{|W_{mmse}Y - X|\}] \tag{16}$$

$$min[E\{(WY - X)(WY - X)^{\sim}\}] \tag{17}$$

$$min[E(WY - X)(Y^{\sim}W^{\sim} - X^{\sim})] \tag{18}$$

$$min[E\{WYY^{\sim}W^{\sim} - WYX^{\sim} - XY^{\sim}W^{\sim} + XX^{\sim}\}] \tag{19}$$

$$\min(WR_{YY}W^{\sim} - WR_{YX} - R_{XY}W^{\sim} + R_{XX}) \tag{20}$$

R_{YY} and R_{XX} represents the auto-correlation of the X and Y, respectively. R_{YX} and R_{XY} are cross-correlation of X and Y, respectively. The minima of a function with respect to a variable can be found by partial differential of the function set to zero.

$$\frac{\partial(WR_{YY}W^{\sim} - WR_{YX} - R_{XY}W^{\sim} + R_{XX})}{\partial W} = 0 \tag{20}$$

$$\frac{\partial T^{\sim}VT}{\partial T} = V^{\sim}T + VT \tag{21}$$

Using equation 21 in equation 20,

$$W = {R_{YY}}^{-1} R_{XY} \tag{22}$$

$$R_{YY} = E\{YY^{\sim}\} \tag{23}$$

$$R_{YY} = E\{(HX + N)(HX + N)^{\sim}\} \tag{24}$$

$$R_{YY} = HP_T H^{\sim} + \sigma^2 I \tag{25}$$

$$R_{YY} = (HH^{\sim} + \sigma^2 I) \tag{26}$$

$$R_{XY} = E(XY^{\sim}) \tag{27}$$

$$R_{XY} = E(X(HX + N)^{\sim}) \tag{28}$$

$$R_{XY} = H^{\sim} \tag{29}$$

The MMSE Equalizer is given as

$$W_{mmse} = (HH^{\sim} + \sigma^2 I)^{-1} H^{\sim} \tag{30}$$

$$W_{mmse} = \left(HH^{\sim} + \frac{1}{\mu} I\right)^{-1} H^{\sim} \tag{31}$$

It can be seen that the MMSE equalizer is a function of the channel H and the noise variance σ^2. If the energy of the transmit signal is considered to be unity equation can be written in terms of μ as in equation 31.

With MMSE equalization N_T independent data streams are obtained. The output SNR of n^{th} sub-stream can be derived in a similar method as that applied to ZF equalizer. It is given as is given as $\gamma_{mmse,n}$ presented in equation 32[12].

$$\gamma_{mmse,n} = \frac{\mu}{\left(\left(HH^{\sim} + \frac{1}{\mu}I\right)^{-1}\right)_{nn}} - 1, \quad 1 \leq n \leq N_T \tag{32}$$

2.8. MAXIMUM LIKELIHOOD (ML) RECEIVER

ML receivers are based on optimal vector decoding and they minimize error probability. ML equalization involves calculation of the Euclidian distance between the estimate $\hat{x}$ and all possible transmitted signals (x) and detection of transmitted signal vector that corresponds to the minimum distance. The complexity of this receiver increases for higher order of modulation schemes.

The design criterion of ML receiver is presented below. The objective of the ML receiver is to minimize the probability of error in decoding the transmitted message that is to minimize $P_e = p(\hat{x} \neq x_i|y(t))$ or to maximize $p(\hat{x} = x_i|y(t))$. Signal constellation points have a one-to-one relation with a transmitted message an equivalent condition is to maximize $p(s_i \text{ sent } |y(t))$. Correspondingly, the decision regions (Z_1,...,Z_N) are seen to be the sub-sets of the signal space and are defined as follows [28].

$$Z_i = \left(y: p(s_i \text{ sent}|y) > p\left(s_j \text{ sent}\middle|y\right) \forall j \neq i\right) \tag{33}$$

2.9. SPINNING OF THE VEHICLE

In this work a case of a spinning body such as a missile is considered as one of the communication entities. Due to the spin there is a change in the relative position of the transmitter and receiver. When transmit and receive antennas face each other the received signal strength reaches a maximum and it decreases with increase in θ, that is the angle of arrival as mentioned in Figure 1.1. Hence, the spin can be modeled as a periodic modulation of the channel gain. A 'sine wave model' to mathematically model the antenna gain as illustrated in Figure 2.9. Here, 'a' is the maximum relative antenna gain, 'b' is the gain offset, ϕ is the angular separation between the antennas and T is the time period of rotation.

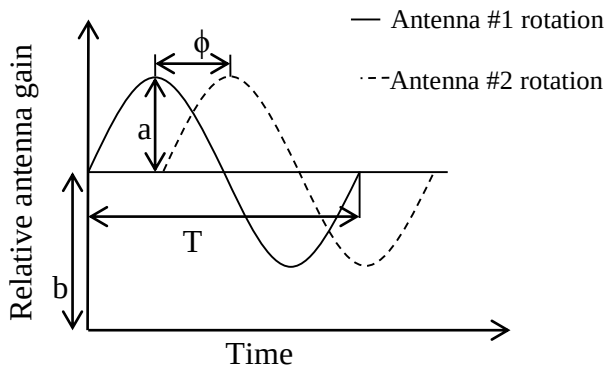

Figure 2.9 Sine Wave Model for Rotation

The variation of relative gain of the antennas mounted on the aero-vehicle is represented in equations 34 and 35.

$$u_1(t) = a + b * \sin(\frac{2\pi}{T} t) \tag{34}$$

$$u_2(t) = a + b * \sin(\frac{2\pi}{T} t) \tag{35}$$

3. SIMULATION RESULTS

3.1. MATLAB SIMULATION

With the availability of advanced computing platforms and robust analysis and simulation tools, computer based simulations have become prevalent means to illustrate and analyze performance of wireless communication systems through the successive stages of development such as conceptualization, design, building of hardware, verification and validation. In this work a simple simulation of the system under consideration is presented. This will mainly serve to check the feasibility of implementation of equalizers to a MIMO system that may be deployed for telemetry communication. MATLAB^{TM}, a technical computing language has been used for simulation and analysis of our model. Figure 3.1 presents the high level block diagram of the simulation model.

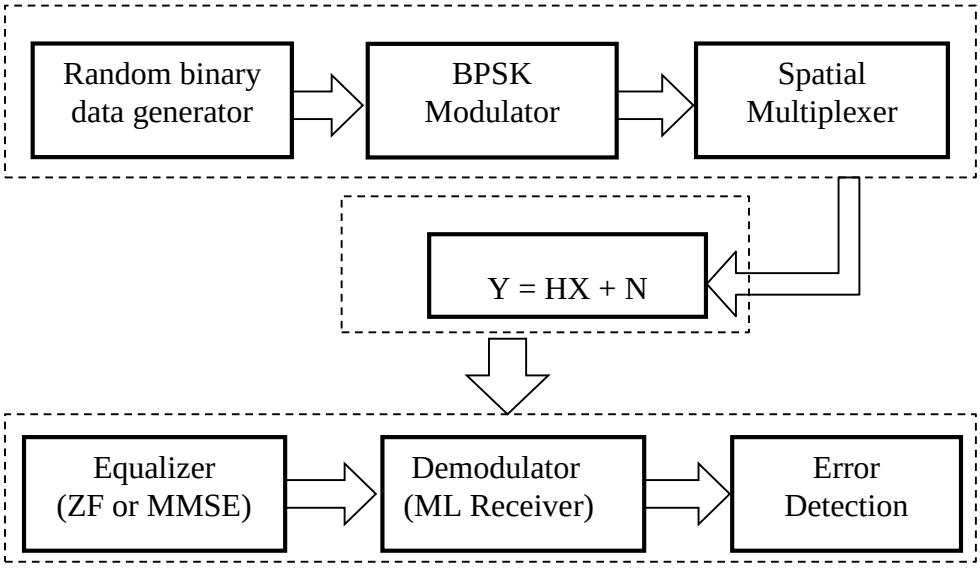

Figure 3.1 Block Diagram of the Simulation Model

3.2. DATA SOURCE

The uniform pseudorandom binary data source generates equally likely bits [0,1].

3.3. BPSK MODULATION

In BPSK modulation, the carrier wave is modulated by changing the phase by π and 0 for the input binary bit '0' and '1', respectively, for each bit interval T_b. To simulate the phase change of π radians for 0 and 1, the binary data 0 and 1 are mapped to -1 and +1, respectively, according to the relation n = 2*m – 1, where m =[0,1].

3.4. SPATIAL MULTIPLEXING

Two modulated symbols are transmitted simultaneously in each STS as a part of independent parallel data streams. In this way, the spatial domain is reused or multiplexed. In accordance with this spatial multiplexing scheme total duration to transmit N bits is N/2 STS or (N/2)*Tb seconds (Tb is the bit interval) thereby increasing the channel capacity by two times.

3.5. AWGN NOISE

The communication systems several undesired noise signals corrupt the information that is transmitted. Some of these include thermal noise (Johnson-Nyquist noise), shot noise and black body radiation. A Gaussian distributed random variable is seen to effectively model the noise.

3.6. CHANNEL

The Rayleigh channel is implemented as a complex vector sum of two independent and identically distributed zero mean Gaussian random variables. The rand function native to MATLAB^{TM} that is used. A pdf distribution of the simulated Rayleigh channel is shown and is compared with a theoretical Rayleigh pdf. It can be seen in Figure 3.2 that the simulated channel closely follows a theoretical Rayleigh distribution.

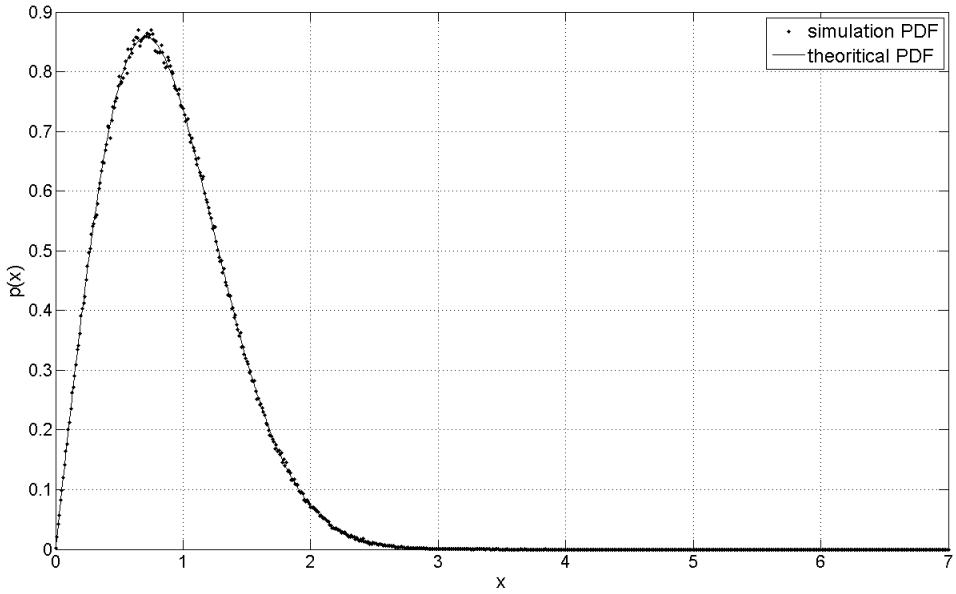

Figure 3.2 Characteristic of a Rayleigh Channel

3.7. EQUALIZATION

It is assumed that the CSI is known to the receiver. The H matrix is updated once in each STS and is used to generate the equalization matrix in accordance with equations 10 and 31, for ZF and MMSE criteria. Note that this process involves matrix inversion. The standard formula for matrix inversion given by equation 36 is used. Alternatively a MATLAB™ command inv can also be implemented for calculation of the inverse.

$$A^{-1} = \frac{A^{\ddagger}}{|A|} \tag{36}$$

Where $A^{\ddagger}$ is the adjoint(A).

3.8. COMPARISON OF ZF AND MMSE EQUALIZERS

In this section, results that compare the performance of the two equalizers are presented. One way to compare the performance is by analysis of the scatter plots of the signal. Figures 3.3 through 3.5 present the scatter plots of at different stages in the receiver.

Comparison of figure with figure and figure shows the action of the equalizer on the received signal vector for a case of BPSK modulation at 20dB SNR. It may be relevant to note that nearly 10^4 bits were transmitted for this experiment to illustrate the behavior of the equalizers. The effect of ISI and noise that is reduced to render the symbols that resemble the transmit signal and effectively equalizing the effect of channel on the signal. The scatter-plot of the output from the zero forcing equalizer is seen to be more dispersed in comparison with MMSE equalizer. This is because of noise amplification by ZF equalizer. The comparison shows that MMSE equalization provides a superior treatment of noise.

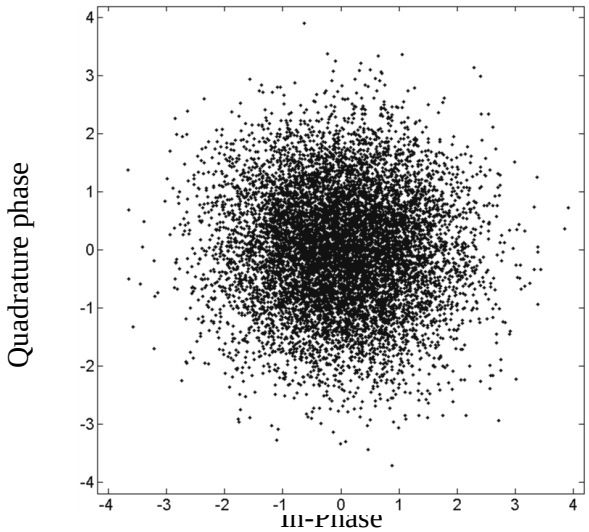

Figure 3.3 Scatter Plot of the Received Signal Prior Equalization at SNR = 20dB

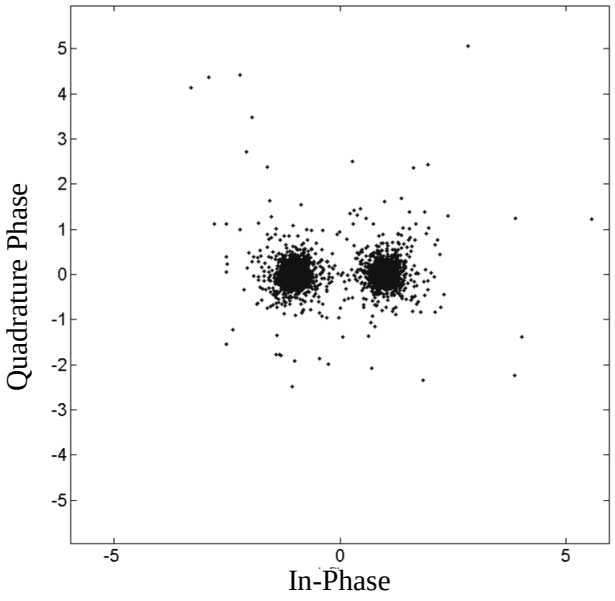

Figure 3.4 Scatter Plot of the Received Signal with ZF Equalization at SNR = 20dB

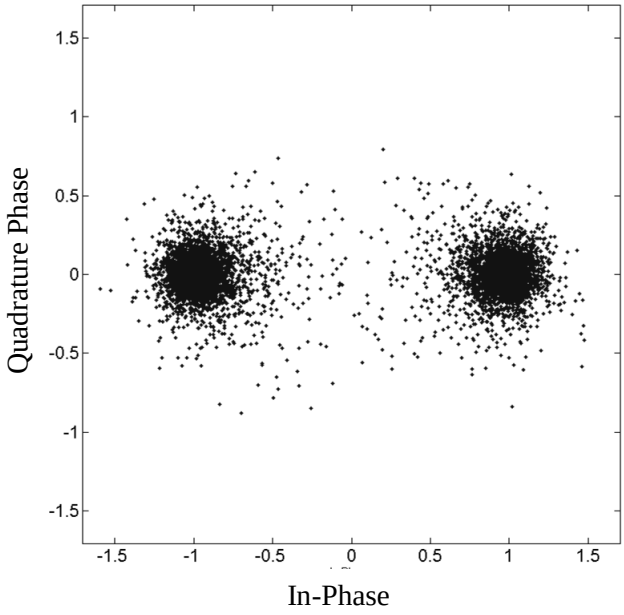

Figure 3.5 Scatter Plot of the Received Signal with MMSE Equalizer (SNR = 20dB)

3.9. MAXIMUM LIKELIHOOD RECEIVER

A ML detector for BPSK is determined based on equation 33. A decision boundary is derived for based on a maximum likelihood condition. For BPSK the decision boundary is along the y = 0 line.

3.10. SPINNING OF THE VEHICLE

In this work, a case of a spinning body such as a missile is considered as one of the communication entities. Due to the spin there is a change in the relative position of

the transmitter and receiver. When transmit and receive antennas face each other the received signal strength reaches a maximum and it decreases with increase in the angle between the antennas. Hence, the spin can be modeled as a periodic modulation of the channel gain.

The effect of rotation is simulated, and the Rayleigh channel is now seen to have a periodic component associated with it. Figures 3.6 through 3.9 show the channel characteristics and a comparison between them shows their trend with respect to SNR.

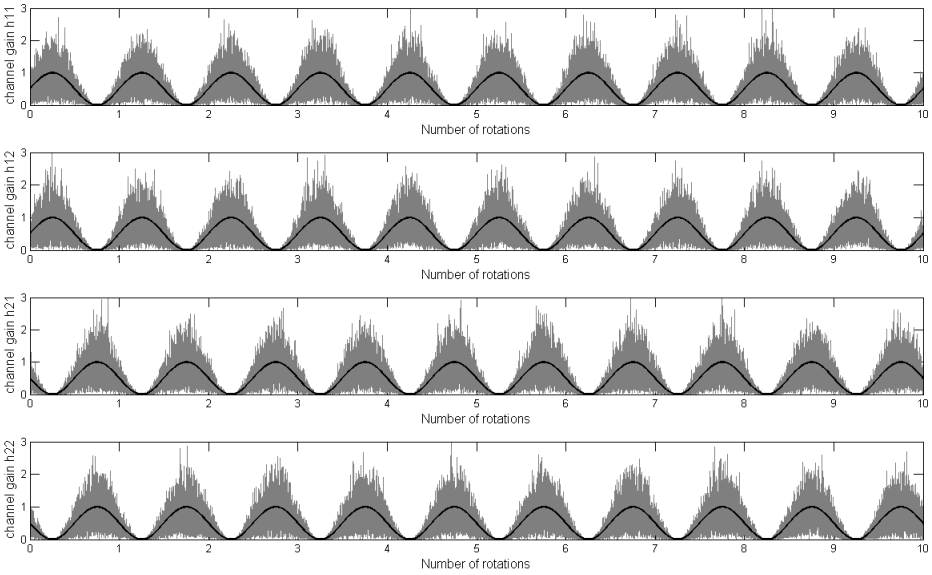

Figure 3.6 Channel Coefficients (Rotating Rx)

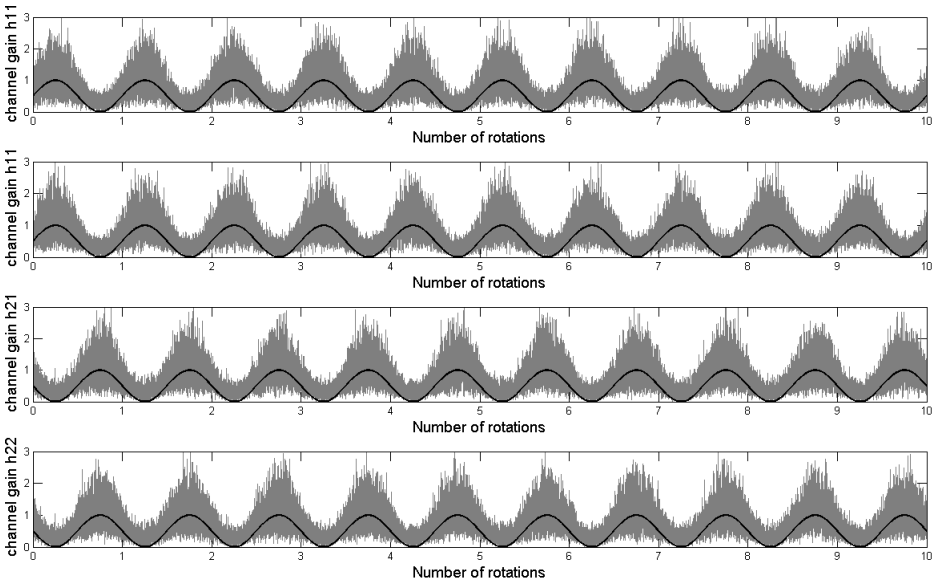

Figure 3.7 Channel Coefficients at SNR = 10dB (Rotating Rx)

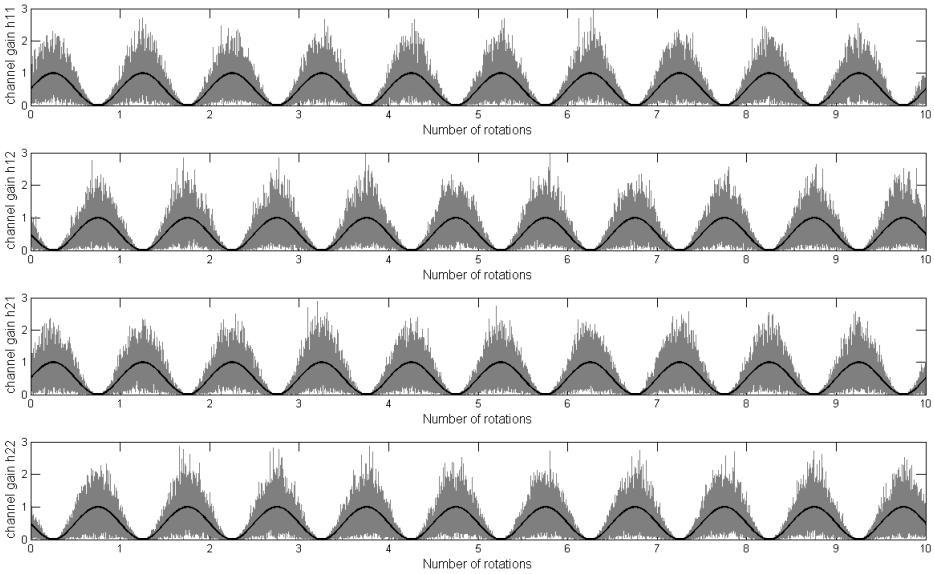

Figure 3.8 Channel Coefficients (Rotating Tx)

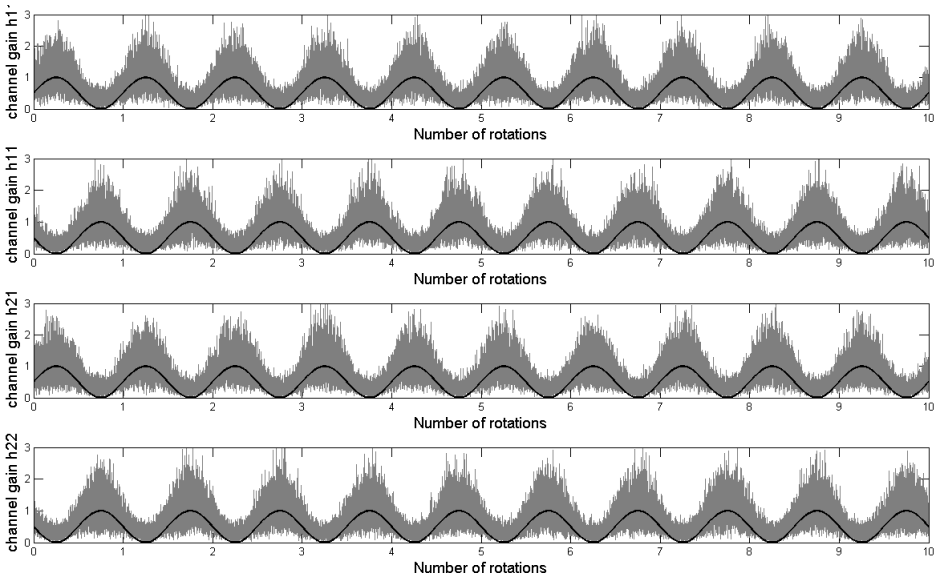

Figure 3.9 Channel Coefficients at SNR = 10dB (Rotating Tx)

4. RESULTS AND DISCUSSIONS

4.1. PERFORMANCE IN A STATIONARY CASE

As a first step the performance of the proposed equalizers is evaluated by considering a scenario where the transmitters and receivers are stationary. Figure 4.1 presents the result for this case. The performance of MMSE equalizer is better than ZF equalizer by nearly 3dB. The results are within one dB of previously established results [11, 12, and 14].

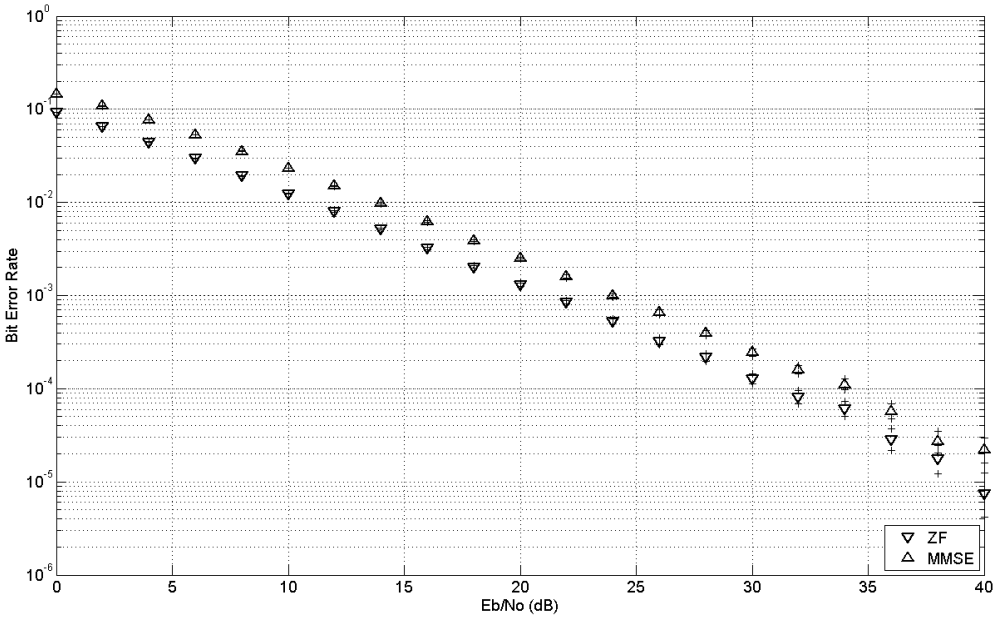

Figure 4.1 Performance of ZF and MMSE for a Stationary Case

4.2. OUTPUT SNR AND PERFORMANCE

In this section, we consider the performance of the MMSE and ZF equalizers in cases of rotating receiver and stationary transmitter, that is the aero-vehicle receives the signal and the base station is the transmitter and rotating transmitter and stationary receiver, that is the aero-vehicle transmits data and the base station is the receiver. A comparative study of performance of equalizers in these cases is presented Based on equation 15 and equation 32 the output SNR of the output streams from the equalizer for cases of stationary transmitter and stationary receiver, rotating transmitter and stationary receiver and rotating receiver and stationary transmitter is obtained. For the stationary case δ_{SNR} saturates to zero. A case of rotating receiver is seen to have similar behavior. However for a case of a rotating transmitter δ_{SNR} increases with increase in SNR. Therefore, in this case, the MMSE equalizer mostly operates in a high SNR regime.

It is seen that the behavior of equalizers for the case where the spinning aero-vehicle is the receiver and the base station is the transmitter follows a trend similar to a case of stationary transmitter and receiver. Therefore, it is expected that the MMSE equalizer would perform better than ZF equalizer with their BER performance curves being parallel to each other. In case of spinning aero-vehicle being the transmitter and the base station being the receiver the trend deviates from the stationary case. In this scenario, the δ_{SNR} increases with increase in SNR at the transmitter. In other words the MMSE equalizer enters into a high SNR regime quicker than the other cases. Therefore, it is expected that the performance of the ZF and MMSE equalizer would merge in this case. A general loss of performance in the two cases of spinning antennas is expected due to loss of power that is transmitted in undesired directions. This loss is more pronounced when the antennas are highly directive. This effect is studied in greater detail in the successive sections. Figure 4.2 presents the trend of difference between SNRs of the output streams with ZF and MMSE equalizers (δ_{SNR}) with a/b set to unity. Figures 4.3 through 4.6 summarize the results discussed in this section.

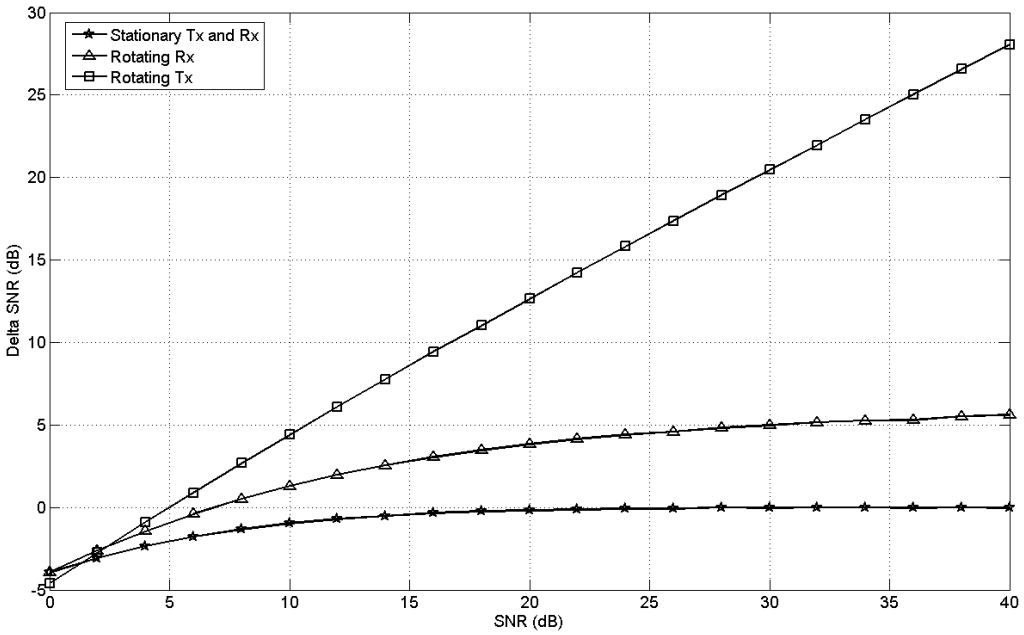

Figure 4.2 Difference between Output SNRs of ZF and MMSE Equalizers

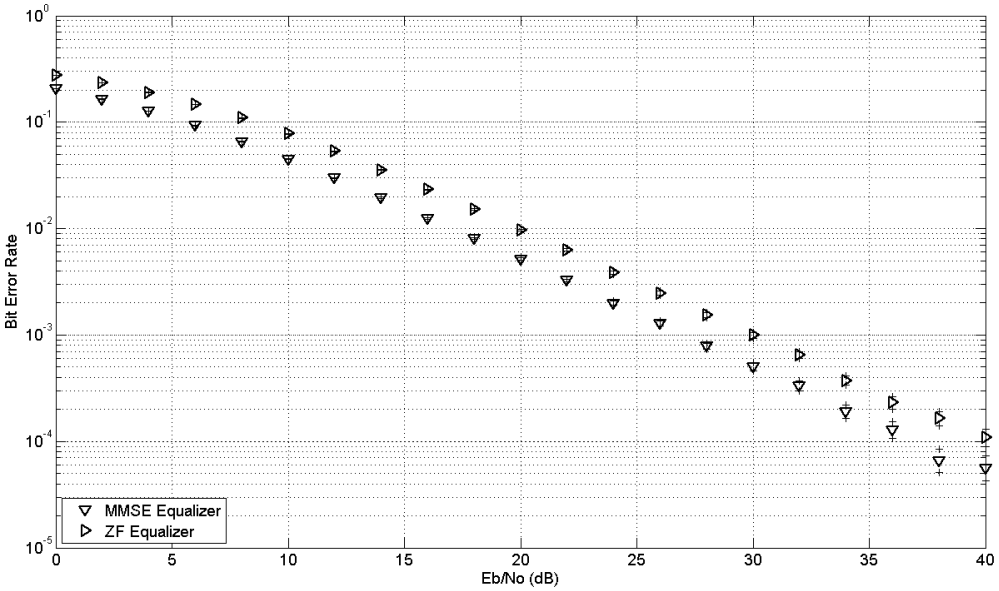

Figure 4.3 BER with Rotating Receivers (a/b = 0)

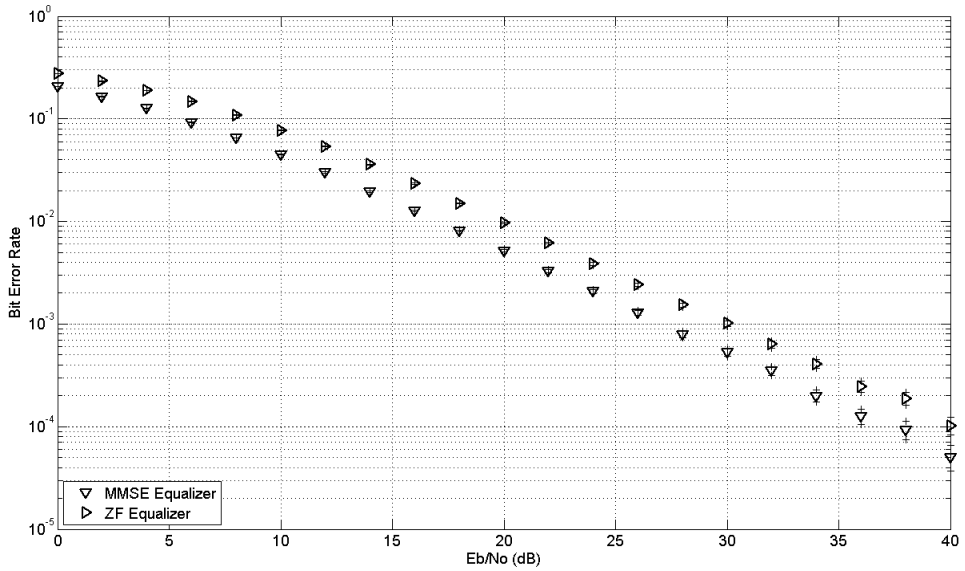

Figure 4.4 BER with Rotating Transmitters (a/b = 0)

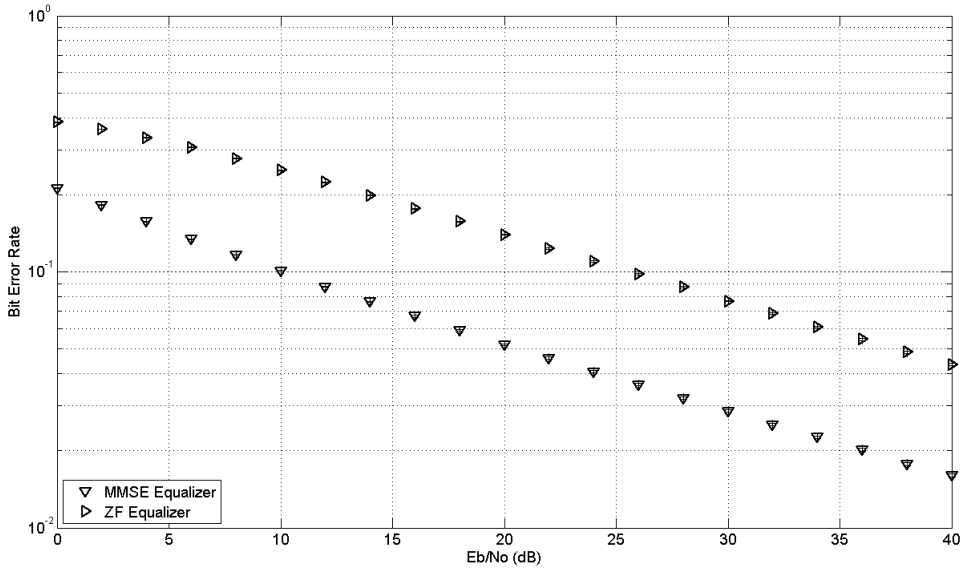

Figure 4.5 BER with Rotating Receivers (a/b = 1)

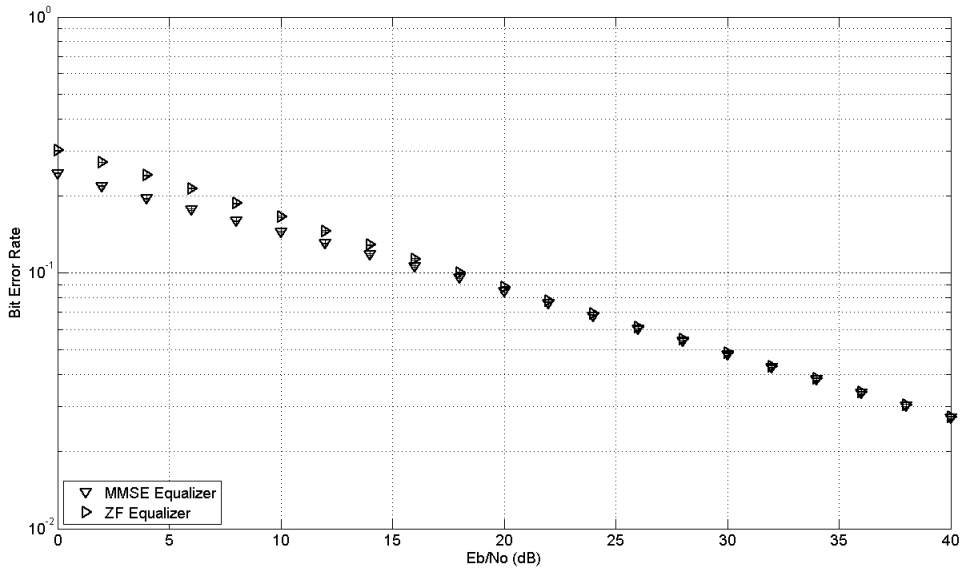

Figure 4.6 BER with Rotating Transmitter (a/b = 1)

4.3. ROTATION AND RELATIVE ANTENNA GAIN

A sine wave model is implemented to simulate the effect of rotation. In the previous section the channel coefficient are verified to have a periodic component corresponding to the frequency of rotation. With increase in a/b ratio there is a more pronounced swing in the relative antenna gain with respect to θ. This means that, with increase in a/b ratio there is an increase in the directivity of the antennas. When a/b is set to zero the antennas are isotropic as seen in Figure 4.7 and the directivity reaches a maximum when a/b is set to unity. This aspect is verified through Figures 4.7 through 4.9.

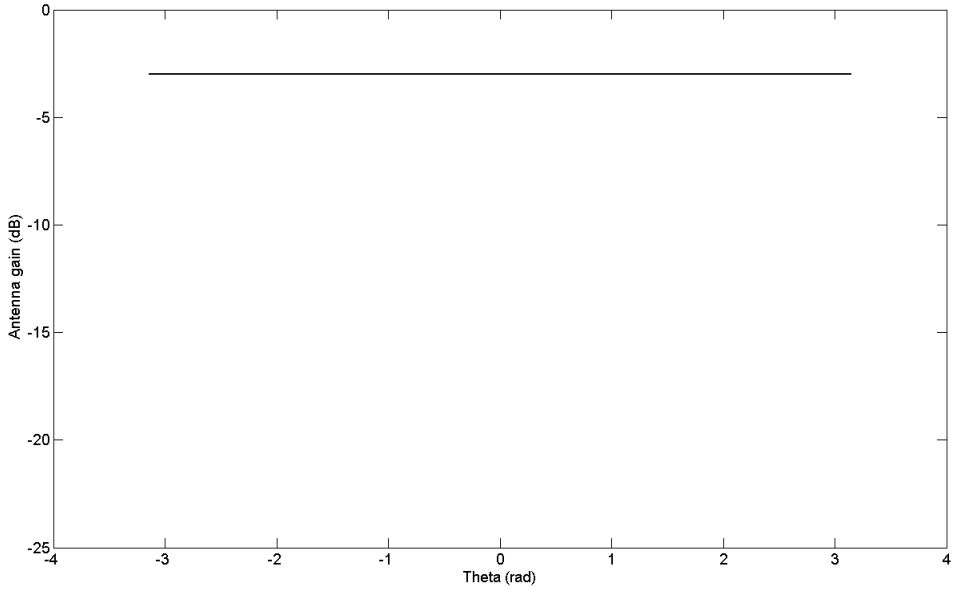

Figure 4.7 Antenna Pattern (a/b = 0)

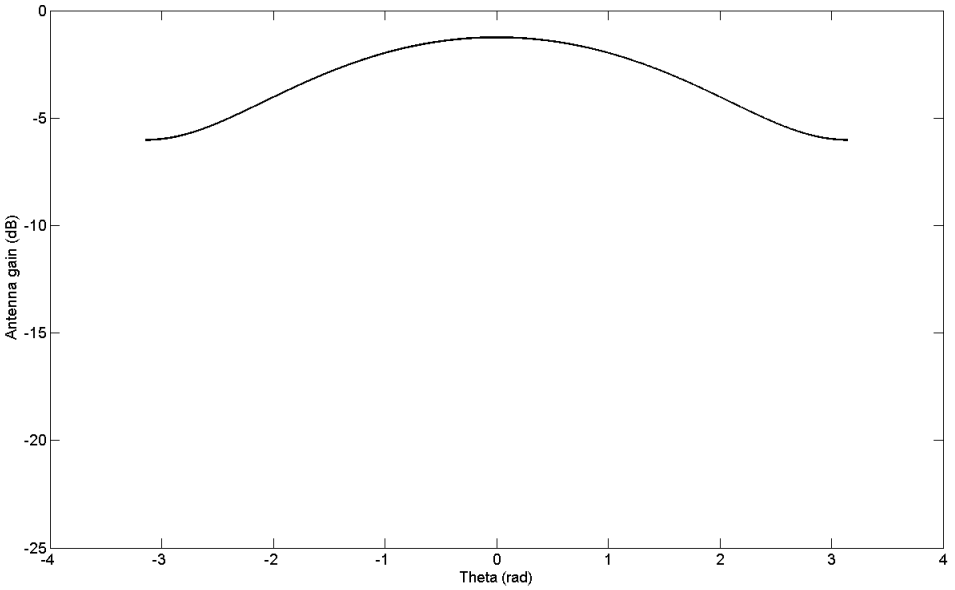

Figure 4.8 Antenna Pattern (a/b = 0.5)

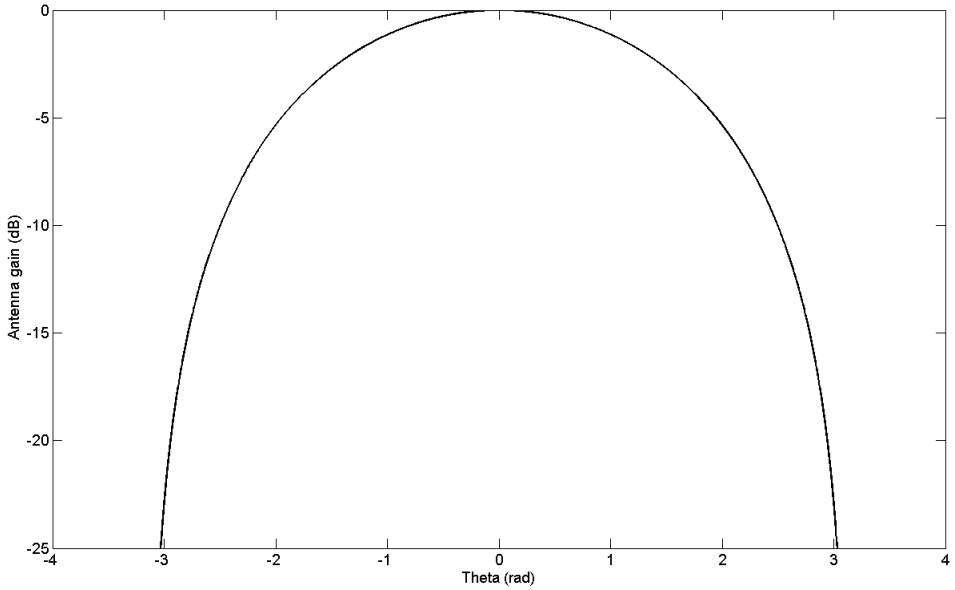

Figure 4.9 Antenna Pattern (a/b = 1)

4.4. DIRECTIVITY AND PERFORMANCE

The effect of directivity on performance of the system in case of one of the communication entities (transmitter or receiver) being a spinning aero-vehicle is studied in this section. The variation of δ_{SNR} with respect to a/b ratio is presented. When the spinning vehicle transmits data and the base station is the receiver it is seen that the receiver is more sensitive to the directivity of the antennas. In this case, the δ_{SNR} increases exponentially with respect to the directivity of the antennas. Figure 4.10 summarizes these results. In accordance with this behavior it is seen that in case of rotating transmitters and stationary receiver MMSE and ZF equalizers tend towards each other as the a//b ratio approaches unity as seen in Figure 4.11. The behavior of equalizers in case of rotating receivers and stationary transmitters can be explained on similar lines. The performance for this case is summarized in Figure 4.12. These results are obtained with SNR set to 25 dB.

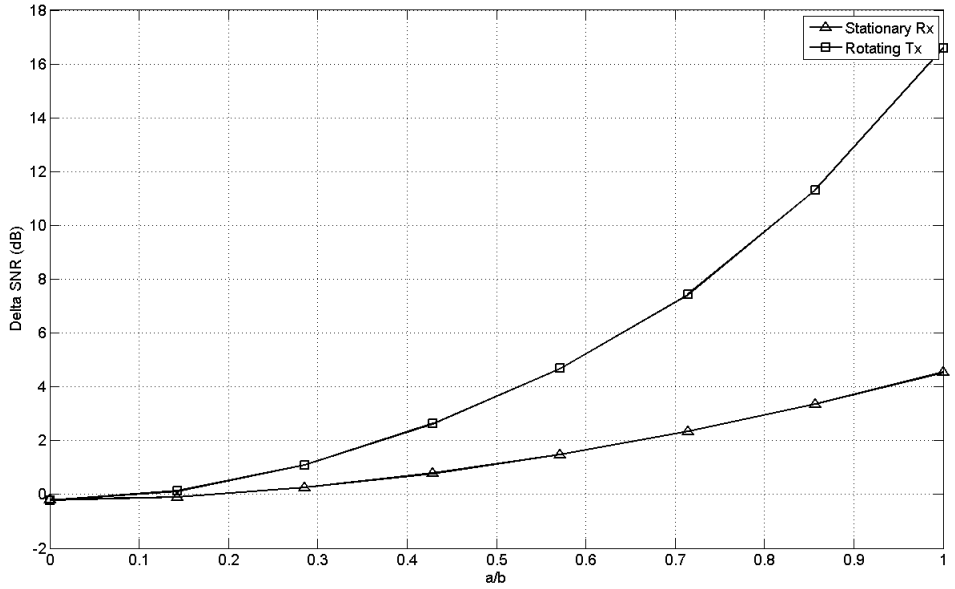

Figure 4.10 Delta SNR with respect to a/b

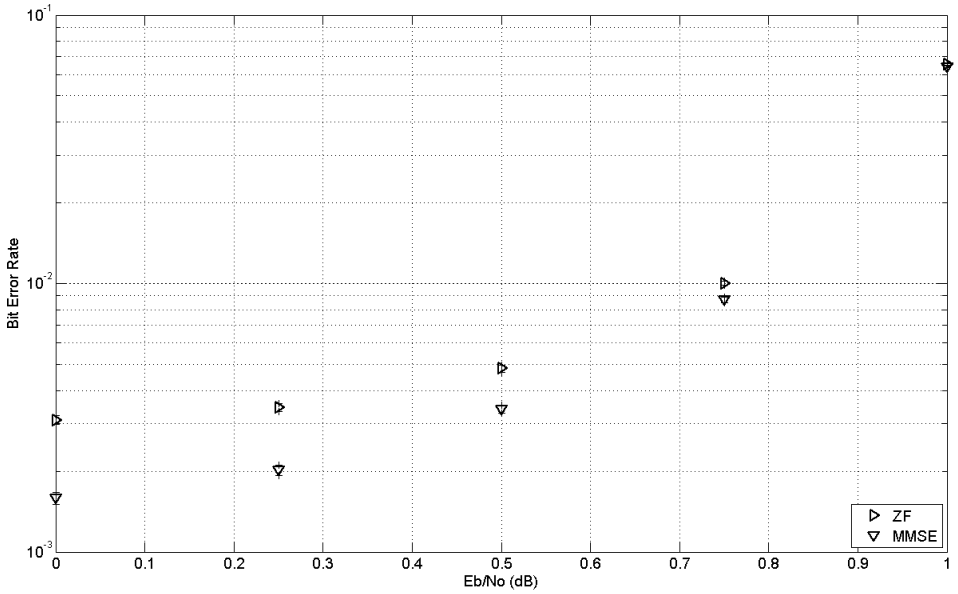

Figure 4.11 BER v/s a/b (Rotating Transmitter)

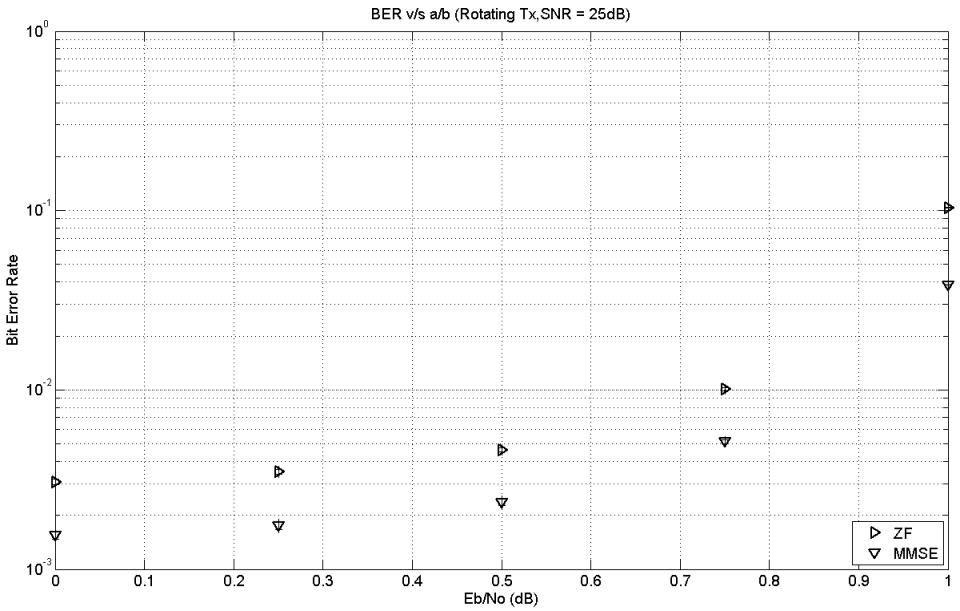

Figure 4.12 BER v/s a/b (Rotating Receiver)

4.5. SNR AND DIRECTIVITY RELATION - ROTATING RX CASE

In the previous section the behavior of equalizers with respect to the dynamics of the system was presented as a comparative study. Now the behavior of the equalizers is studied for a case of the spinning vehicle being the receiver. In this case, the system consists of a rotating receiver and a stationary transmitter

Figures 4.13 and 4.14 summarize the behavior of MMSE and ZF equalizer. For lower SNR it is seen that there is no significant effect of increase in antenna directivity. However at higher SNR the system is highly sensitive to change in directivity of the antenna. It is also seen that when a/b is set to unity the performance gain that can be achieved by increasing SNR is negligible. So for practical purposes the performance becomes quite independent of variation in SNR for systems with highly directive antenna.

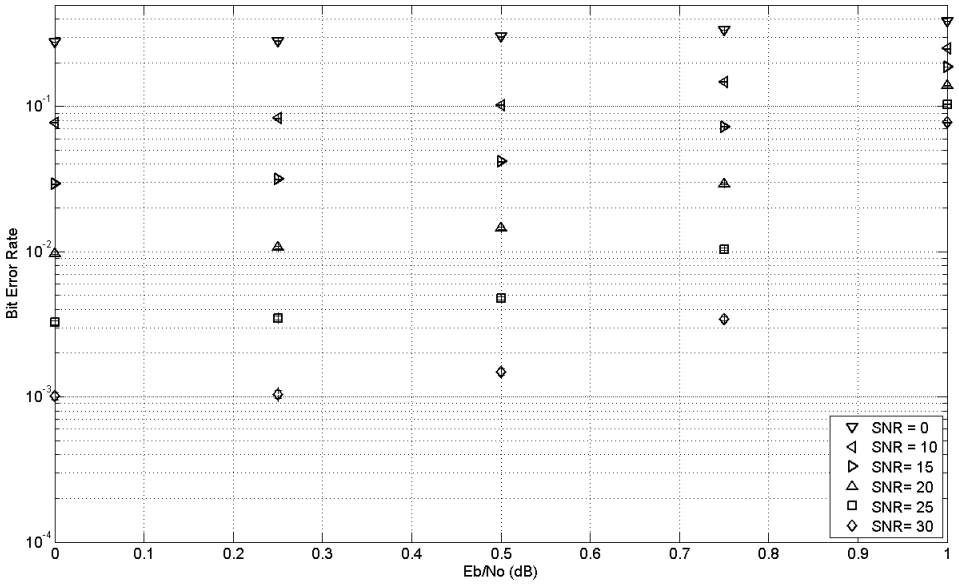

Figure 4.13 Effect of Relative Antenna Gain on ZF (Rotating Rx)

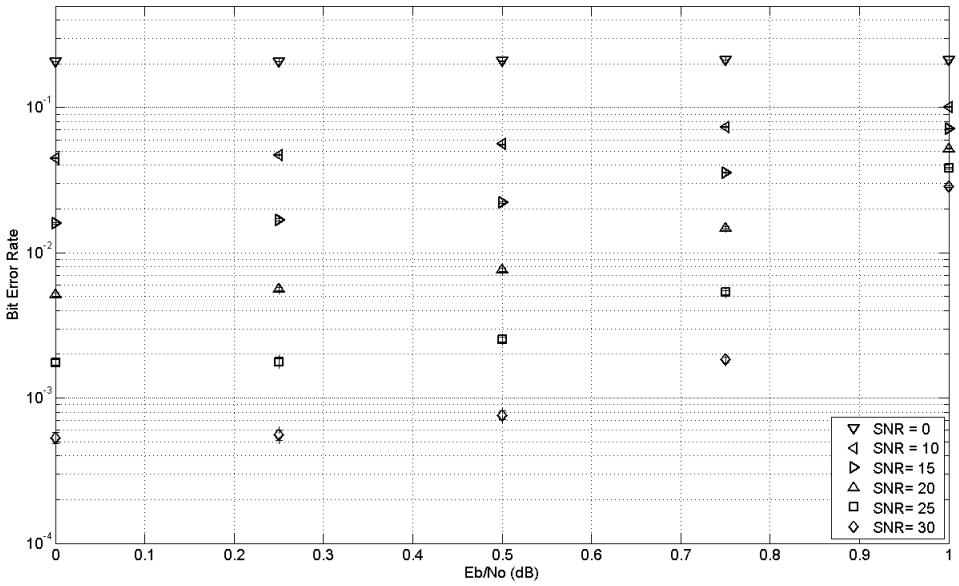

Figure 4.14 Effect of Relative Antenna Gain on MMSE (Rotating Rx)

4.6. SNR AND DIRECTIVITY RELATION - ROTATING TX CASE

In this section, the effect of directivity of the antenna when the spinning aero-vehicle is the transmitter is presented. BER is seen to increase with a/b ratio for both ZF and MMSE equalizers. The increase in BER is dominant at high SNRs. As a/b approaches unity the performance of the equalizers become less dependent on SNR. The trend is similar to the rotating receiver case. These results are summarized in Figures 4.15 and 4.16.

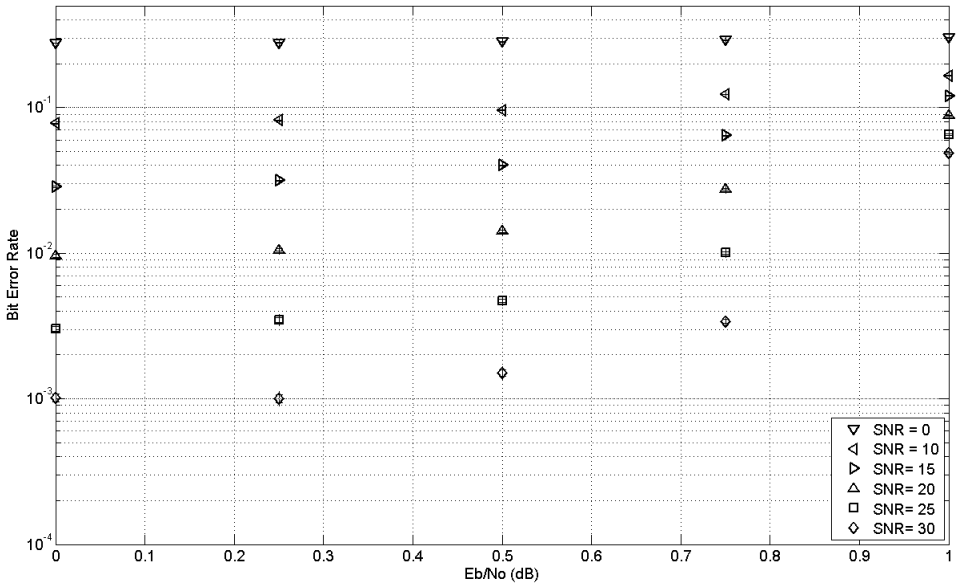

Figure 4.15 Effect of Relative Antenna Gain on ZF Equalizer

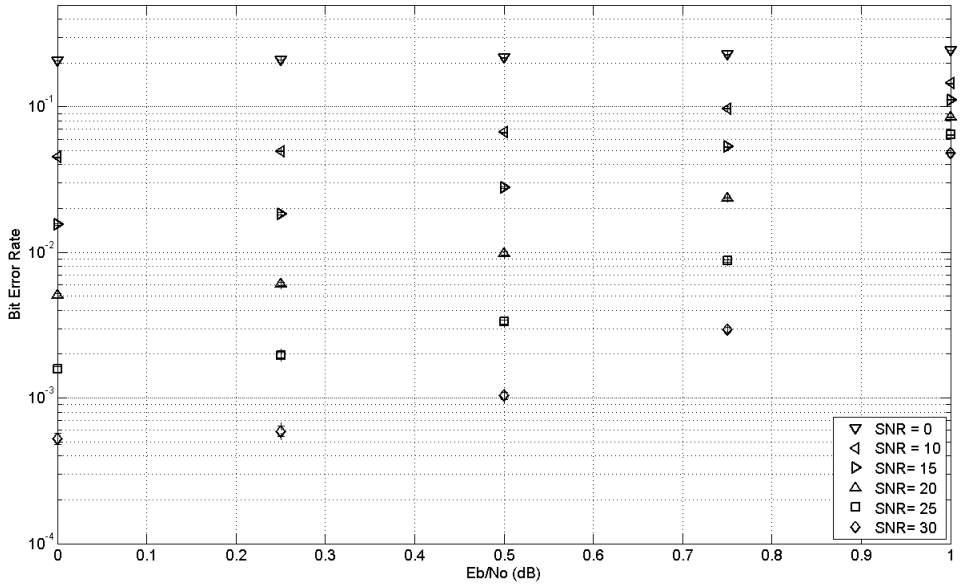

Figure 4.16 Effect of Relative Antenna Gain on MMSE Equalizer

4.7. EFFECT OF ANGULAR SEPARATION - ROTATING RX CASE

In the 2x2 MIMO system that has been considered one of the communication entities is a spinning vehicle that is assumed to have a cylindrical geometry. The configuration of the antennas or the angular separation between the antennas placed on the spinning vehicle (ϕ) is seen to affect the performance of the system. This is studied in two sections. In this section, the effect of angular separation between the antennas when the spinning aero-vehicle is the receiver is presented. Figures 4.17 and 4.18 consider two cases of angular separation that are $\phi = 0$ radians and $\phi = \pi$ radians. With the antennas placed laterally the loss of visibility is minimized. There is an improvement in performance when the antennas are placed π radians apart. The a/b ratio is set to unity for this experiment.

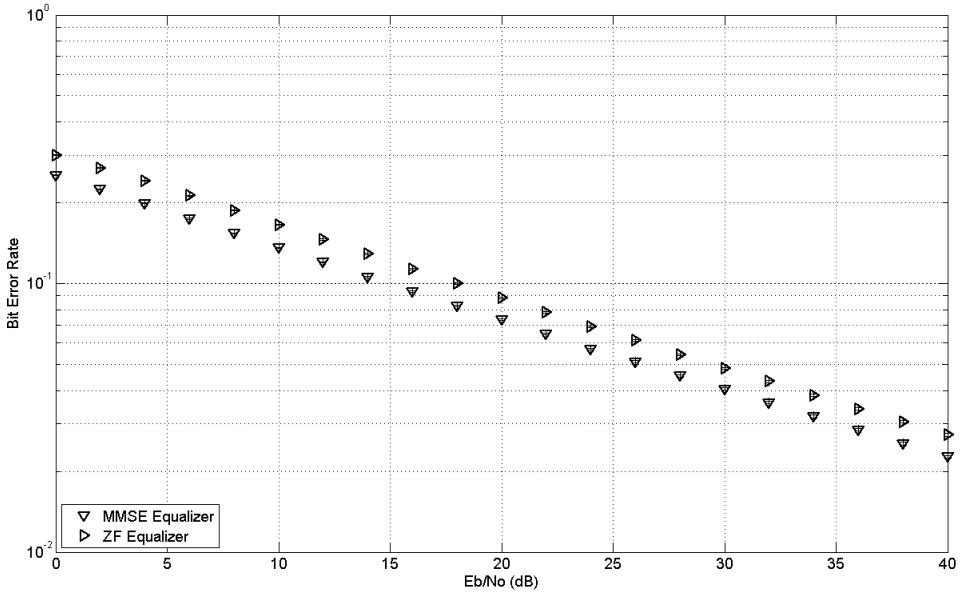

Figure 4.17 BER Performance (a/b = 1, ϕ = 0)

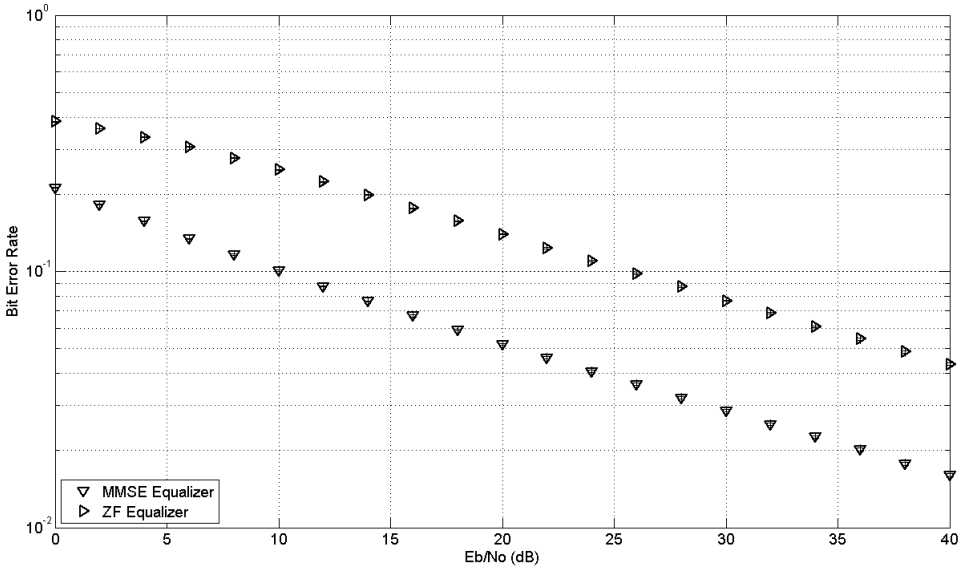

Figure 4.18 BER Performance (a/b = 1, ϕ = 180)

4.8. EFFECT OF ANGULAR SEPARATION FOR ROTATING TX

An experiment similar to the previous section is set up in this section. In this section, the effect of angular separation between the antennas when the spinning aero-vehicle is the transmitter is presented. Figures 4.19 - 4.21 show that the performance of MMSE and ZF equalizer tend towards each other with increase in angular separation between the antennas.

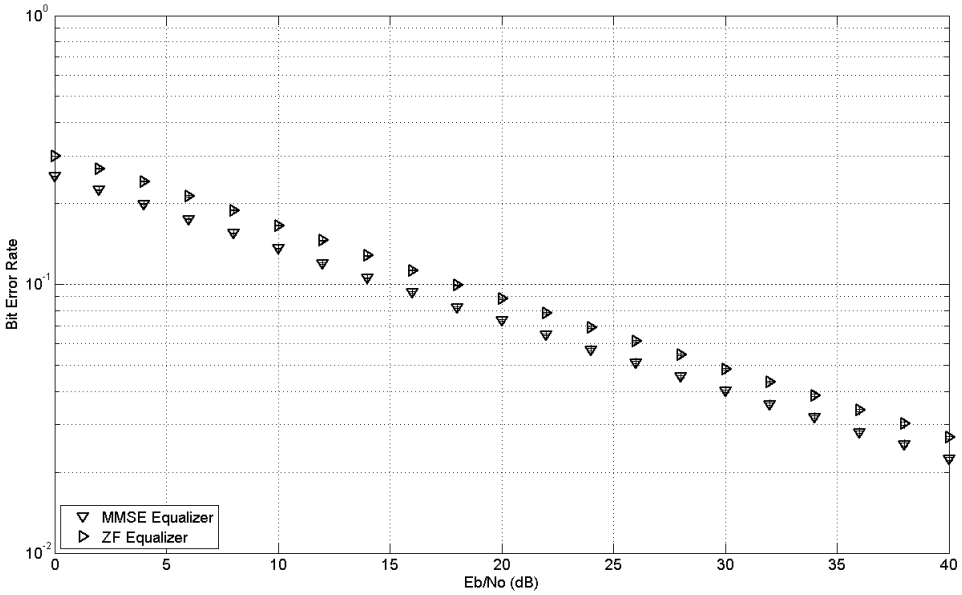

Figure 4.19 BER Performance (a/b =1, ϕ = 0)

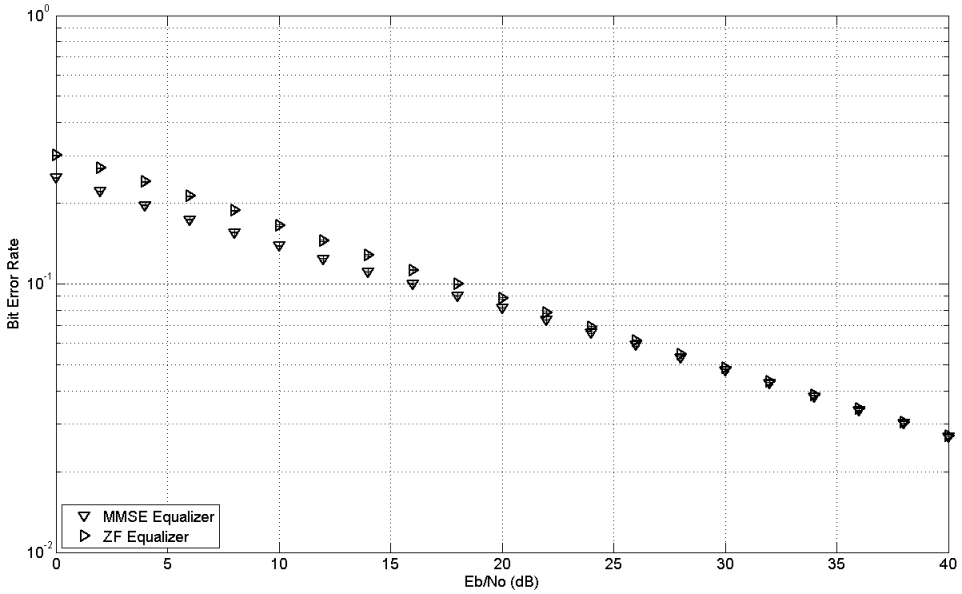

Figure 4.20 BER Performance (a/b =1, ϕ = 90)

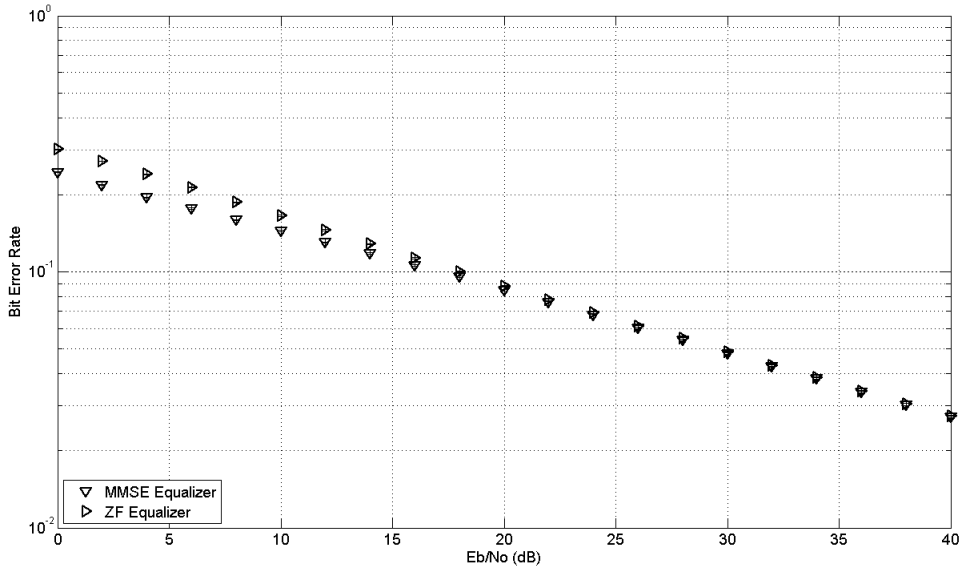

Figure 4.21 BER Performance (a/b =1, ϕ = 180)

4.9. DESIGN OPTIMIZATIONS

The behavior ZF and MMSE equalizer in a case of full-duplex communication is studied with one of the communication entities being a spinning aero-vehicle. The performance is dictated by the SNR of the output streams from the equalizers. Based on these observations a few important design optimizations are proposed.

4.9.1. Choice of Equalizers. Figure 4.22 illustrates the performance gain of MMSE equalizer in the cases of rotating Rx and stationary Tx and rotating Tx and stationary Rx. This experiment was conducted with a/b set to unity. It is seen that there is no significant gain in performance with use of MMSE equalizer for a case of rotating transmitter.

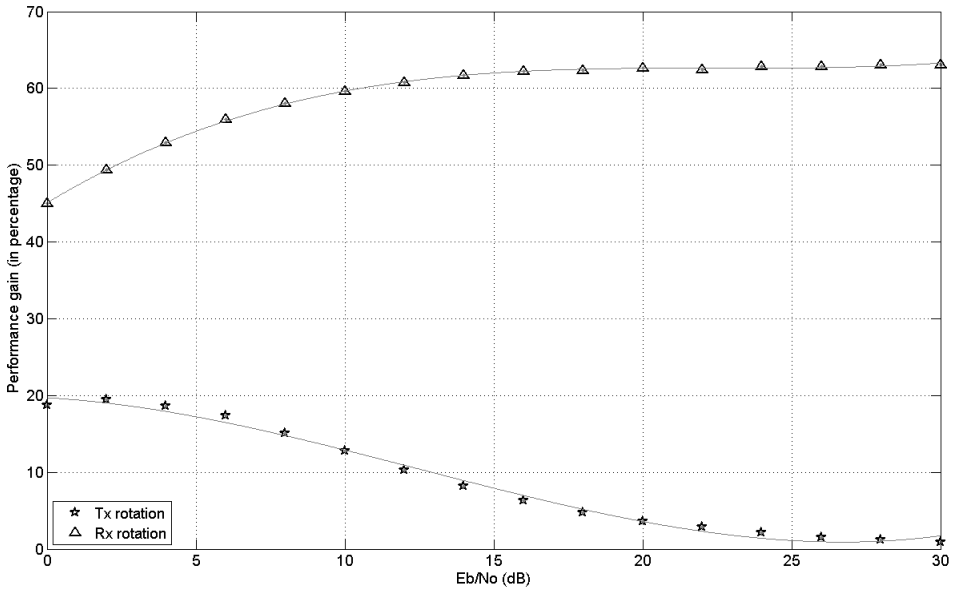

Figure 4.22 Performance Gain in MMSE Equalizer

It was seen that for a case of rotating receiver MMSE performs better than ZF equalizer. However for a case of rotating transmitter the performance of both equalizers closely follow each other. Therefore, at the ground station ZF equalizer can be deployed without any loss of performance. This is useful since with ZF equalizer the knowledge of noise statistics is not required. Figure 4.23 and Figure 4.24 illustrate the optimized receiver architecture for the rotating aero-vehicle and the base station, respectively.

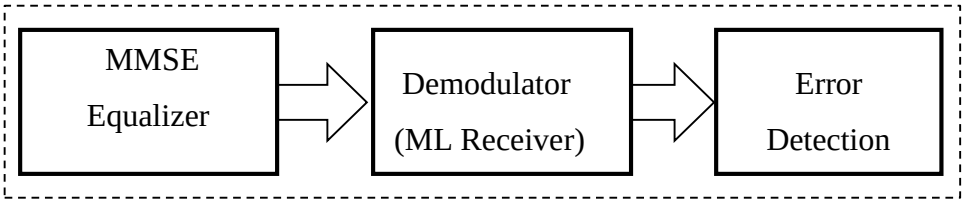

Figure 4.23 Receiver Block Diagram for Spinning Vehicle

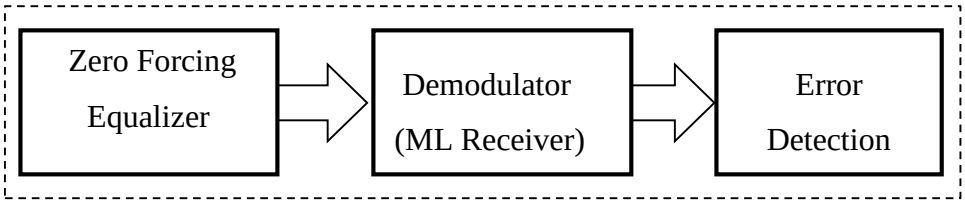

Figure 4.24 Receiver Block Diagram for Base Station

4.9.2. Transmit Power Optimization. From Figures 4.13, 4.14, 4.17 and 4.18 it is seen as the directivity of the antenna increases, the performance drops even though the transmitted power is maintained at the same value. When a/b ratio approaches unity the performance is almost independent of SNR. It is seen that at higher SNR the system is more sensitive to increase in directivity of the antennas. These results are summarized in Figures 4.25 and 4.26 for the cases of rotating receiver and rotating transmitter, respectively. The improved receiver architecture proposed in the previous section is considered in this analysis. Consequently the behavior of MMSE equalizer is studied for a case of rotating transmitters and the performance of ZF equalizer is studied for a case of rotating receiver.

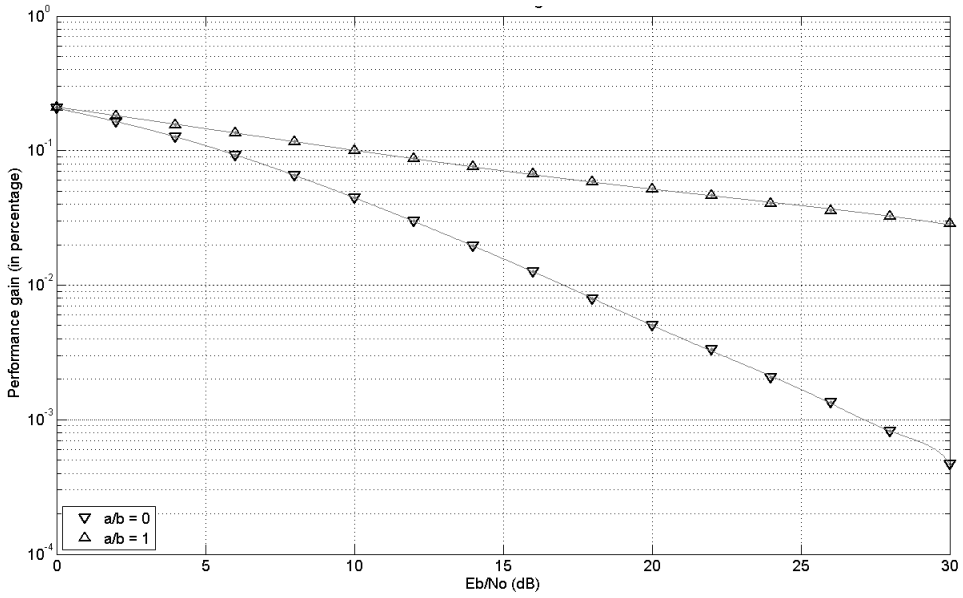

Figure 4.25 Effect of Directivity of Antennas (Rotating Receiver)

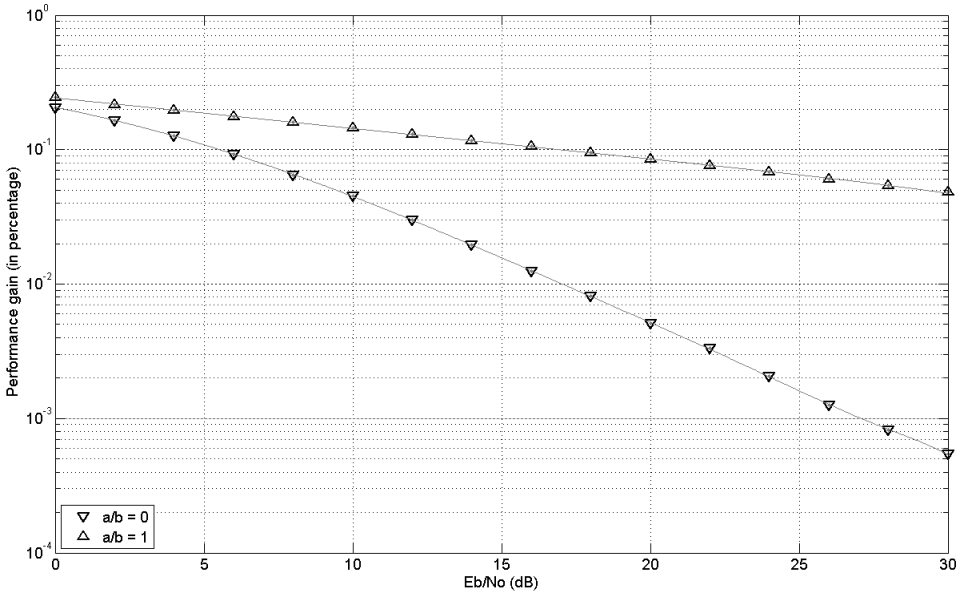

Figure 4.26 Effect of Directivity of Antennas (Rotating Transmitter)

4.9.3. Antenna Configuration. From Figure 4.15 and Figure 4.16 antenna separation of 180 degrees is seen to increase performance when the spinning vehicle is the receiver. At this configuration, when the rotating body behaves as a transmitter the performance of ZF equalizer tends closer towards the MMSE equalizer. This allows to use deploy the receiver architecture discussed in Section 4.9.1.Thereby allowing optimization at the transmitter and receiver ends.

5. CONCLUSION

In this thesis, ZF and MMSE equalizers based on a BLAST architecture has been formulated for a 2X2 MIMO system. A theoretical framework to predict the performance of the equalizers is proposed and verified. The model is checked for consistency by verifying its performance for a static case. Further, the performance is studied for a case in which one of the communication entities is mounted on a spinning vehicle. The effect of directivity and angular placement of antennas is studied. It is seen that the BER increases with increase in directivity of the antenna. Also in such a case the performance of MMSE equalizer closely follows ZF equalizer. Hence, for systems with highly directive antennas a ZF equalizer can replace MMSE. Also with increase in antenna directivity the MIMO systems are less sensitive to SNR. Hence, with our observations we suggest that for a/b set to unity lower SNRs can be preferred. It is also proved that antenna placed diametrically opposite on a rotating body is the best solution. Based on the simulation results new design optimizations are proposed. The proposed model is seen to have reduced complexity and computation, smart choice of transmits power and optimal placement of antennas on the spinning vehicle. In the background of the challenging conditions that demand robust solutions for effective communication this work can be seen to be a relevant contribution in the field of aerospace telemetry

APPENDIX A

EQUALIZATION FOR A STATIONARY RX AND TX

```
%=========================================================================
% ZF and MMSE Equalization for a 2x2 MIMO with spatial multiplexing
% Ver. Date: 06/11/2014
%=========================================================================


% --------------------- PARAMETERS: ----------------------------------
% N = Number of Symbols for experiment
% SNR_dB = Signal-to-Noise Ration in dB
% num_Tx = Number of transmit antennas
% num_Rx = Number of receive antennas
%-------------------------------------------------------------------------

clear all;close all hidden;clc
N = 1e6; % Number of bits
SNR_dB = [0:2:40];
num_Rx = 2; % Number of receivers
num_Tx = 2; % number of transmitters

for SNRcounter = 1:length(SNR_dB)

    % Generate random binary data
    bits = rand(1,N)>0.5; % creates 0s and 1s with equal probability
    BPSK_symbols = 2*bits-1; % generate  BPSK symbols

    %grouping the symbols in accordance with Spatial Multiplexing
    %techinique
    seq = repmat(BPSK_symbols,[num_Tx 1]);

    % Generate slow fading rayleigh coefficients
    h = 1/sqrt(2)*[randn(num_Tx,N) + 1j*randn(num_Tx,N)];

    % Model AWGN with 0dB variance
    n = 1/sqrt(2)*[randn(num_Tx,N/num_Tx) + 1j*randn(num_Tx,N/num_Tx)];

    % Y = HX + N
    y_add = zeros(size(seq,1),size(seq,2));
    y_temp = h.*seq;
    y_add(:,1:2:end) = y_temp(:,2:2:end);
    y_add = y_add + y_temp;
    y = y_add(:,1:2:end);

    y = y + 10^(-SNR_dB(SNRcounter)/20)*n;

    % Receiver with ZF Equalization
    h_conj = conj(h);
    h_hermitian = h_conj;
    h_hermitian(2,1:2:end) = h_conj(1,2:2:end);
    h_hermitian(1,2:2:end) = h_conj(2,1:2:end);

    h_3d = reshape(h,[2,2,N/num_Tx]);
    h_conj_3d = reshape(h_conj,[2,2,N/num_Tx]);
    h_hermitian_3d = reshape(h_hermitian,[2,2,N/num_Tx]);
    y_3d = reshape(y,[2,1,N/num_Tx]);
```

```
    h_herm_h(1,1,:) = sum(h_conj_3d(:,1,:).*h_3d(:,1,:),1);
    h_herm_h(1,2,:) = sum(h_conj_3d(:,1,:).*h_3d(:,2,:),1);
    h_herm_h(2,1,:) = sum(h_conj_3d(:,2,:).*h_3d(:,1,:),1);
    h_herm_h(2,2,:) = sum(h_conj_3d(:,2,:).*h_3d(:,2,:),1);

    hh_adjoint(1,1,:) = h_herm_h(2,2,:);
    hh_adjoint(1,2,:) = -h_herm_h(1,2,:);
    hh_adjoint(2,1,:) = -h_herm_h(2,1,:);
    hh_adjoint(2,2,:) = h_herm_h(1,1,:);

    hh_determinant = (hh_adjoint(1,1,:).*hh_adjoint(2,2,:) -
hh_adjoint(1,2,:).*hh_adjoint(2,1,:));
    hh_determinant = repmat(hh_determinant,[2,2,1]);

    hh_inverse = hh_adjoint./hh_determinant;

    hhy(1,1,:) = sum((h_conj_3d(:,1,:).*y_3d),1);
    hhy(2,1,:) = sum((h_conj_3d(:,2,:).*y_3d),1);

    hh_inverse_mul = hh_inverse;
    hh_inverse_mul(2,1,:) = hh_inverse(1,2,:);
    hh_inverse_mul(1,2,:) = hh_inverse(2,1,:);

    y_estimate(1,1,:) = sum((hh_inverse_mul(:,1,:).*hhy),1);
    y_estimate(2,1,:) = sum((hh_inverse_mul(:,2,:).*hhy),1);

    bits_estimate = real(y_estimate) > 0;

    bits_est = reshape(bits_estimate,[1,N]);

    err_ZF(SNRcounter) = sum(abs([bits - bits_est]));

    %MMSE Equalizer
    hh_adjoint(1,1,:) = h_herm_h(2,2,:) + 10^(-SNR_dB(SNRcounter)/10);
    hh_adjoint(1,2,:) = -h_herm_h(1,2,:);
    hh_adjoint(2,1,:) = -h_herm_h(2,1,:);
    hh_adjoint(2,2,:) = h_herm_h(1,1,:) + 10^(-SNR_dB(SNRcounter)/10);

    hh_determinant = (hh_adjoint(1,1,:).*hh_adjoint(2,2,:) -
hh_adjoint(1,2,:).*hh_adjoint(2,1,:));
    hh_determinant = repmat(hh_determinant,[2,2,1]);

    hh_inverse = hh_adjoint./hh_determinant;

    hhy(1,1,:) = sum((h_conj_3d(:,1,:).*y_3d),1);
    hhy(2,1,:) = sum((h_conj_3d(:,2,:).*y_3d),1);

    hh_inverse_mul = hh_inverse;
    hh_inverse_mul(2,1,:) = hh_inverse(1,2,:);
    hh_inverse_mul(1,2,:) = hh_inverse(2,1,:);

    y_estimate(1,1,:) = sum((hh_inverse_mul(:,1,:).*hhy),1);
    y_estimate(2,1,:) = sum((hh_inverse_mul(:,2,:).*hhy),1);
```

```
    bits_estimate = real(y_estimate) > 0;

    bits_est = reshape(bits_estimate,[1,N]);

    err_MMSE(SNRcounter) = sum(abs([bits - bits_est]));

end

Calc_ber_ZF = err_ZF/N;
Calc_ber_MMSE = err_MMSE/N;
```

APPENDIX B

EQUALIZATION FOR A SPINNING VEHICLE

```
%=========================================================================
% ZF and MMSE Equalization for a 2x2 MIMO with spatial multiplexing
% Author: Aditya Kulkarni
% Ver. Date: 06/11/2014
%=========================================================================

% --------------------- PARAMETERS: ----------------------------------
% N = Number of Symbols for experiment
% SNR_dB = Signal-to-Noise Ratio in dB
% num_Tx = Number of transmit antennas
% num_Rx = Number of receive antennas
% a = maximum  swing in the antenna gain
% b = antenna gain offset
% phi = angular separation between the antennas
% l = Controls the rate of rotation of the aero-vehicle
%-------------------------------------------------------------------------

clear all;close all hidden;clc
N = 1e6; % Number of bits
SNR_dB = [0:2:40];
num_Rx = 2; % Number of receivers
num_Tx = 2; % number of transmitters
b = 0.5;
a = 0.5;


for SNRcounter = 1:length(SNR_dB)

    % Generate random binary data
    bits = rand(1,N)>0.5; % creates 0s and 1s with equal probability
    BPSK_symbols = 2*bits-1; % generate  BPSK symbols

    %grouping the symbols in accordance with Spatial Multiplexing
    %techinique
    seq = repmat(BPSK_symbols,[num_Tx 1]);

    % Generate slow fading rayleigh coefficients
    h = 1/sqrt(2)*[randn(num_Tx,N) + 1j*randn(num_Tx,N)];


    % Rotation of the aero-vehicle
    l = N/2;
    pt = 1:N/2;
    phi = pi;
    phi_arr = phi.*ones(1,l);

    sin_tx1 = b + a.*sin(2*pi*(100/l).*pt);
    sin_tx2 = b + a.*sin((2*pi*(100/l).*pt)+phi_arr);

    h(1,1:2:end) = h(1,1:2:end).*sin_tx1;
    h(1,2:2:end) = h(1,2:2:end).*sin_tx2;
    h(2,1:2:end) = h(2,1:2:end).*sin_tx1;
    h(2,2:2:end) = h(2,2:2:end).*sin_tx2;
```

```
    % Model AWGN with 0dB variance
    n = 1/sqrt(2)*[randn(num_Tx,N/num_Tx) + 1j*randn(num_Tx,N/num_Tx)];

    % Y = HX + N
    y_add = zeros(size(seq,1),size(seq,2));
    y_temp = h.*seq;
    y_add(:,1:2:end) = y_temp(:,2:2:end);
    y_add = y_add + y_temp;
    y = y_add(:,1:2:end);

    y = y + 10^(-SNR_dB(SNRcounter)/20)*n;

    % Receiver with ZF Equalization
    h_conj = conj(h);
    h_hermitian = h_conj;
    h_hermitian(2,1:2:end) = h_conj(1,2:2:end);
    h_hermitian(1,2:2:end) = h_conj(2,1:2:end);

    h_3d = reshape(h,[2,2,N/num_Tx]);
    h_conj_3d = reshape(h_conj,[2,2,N/num_Tx]);
    h_hermitian_3d = reshape(h_hermitian,[2,2,N/num_Tx]);
    y_3d = reshape(y,[2,1,N/num_Tx]);

    h_herm_h(1,1,:) = sum(h_conj_3d(:,1,:).*h_3d(:,1,:),1);
    h_herm_h(1,2,:) = sum(h_conj_3d(:,1,:).*h_3d(:,2,:),1);
    h_herm_h(2,1,:) = sum(h_conj_3d(:,2,:).*h_3d(:,1,:),1);
    h_herm_h(2,2,:) = sum(h_conj_3d(:,2,:).*h_3d(:,2,:),1);

    hh_adjoint(1,1,:) = h_herm_h(2,2,:);
    hh_adjoint(1,2,:) = -h_herm_h(1,2,:);
    hh_adjoint(2,1,:) = -h_herm_h(2,1,:);
    hh_adjoint(2,2,:) = h_herm_h(1,1,:);

    hh_determinant = (hh_adjoint(1,1,:).*hh_adjoint(2,2,:) -
hh_adjoint(1,2,:).*hh_adjoint(2,1,:));
    hh_determinant = repmat(hh_determinant,[2,2,1]);

    hh_inverse = hh_adjoint./hh_determinant;

    hhy(1,1,:) = sum((h_conj_3d(:,1,:).*y_3d),1);
    hhy(2,1,:) = sum((h_conj_3d(:,2,:).*y_3d),1);

    hh_inverse_mul = hh_inverse;
    hh_inverse_mul(2,1,:) = hh_inverse(1,2,:);
    hh_inverse_mul(1,2,:) = hh_inverse(2,1,:);

    y_estimate(1,1,:) = sum((hh_inverse_mul(:,1,:).*hhy),1);
    y_estimate(2,1,:) = sum((hh_inverse_mul(:,2,:).*hhy),1);

    bits_estimate = real(y_estimate) > 0;

    bits_est = reshape(bits_estimate,[1,N]);
```

```
    err_ZF(SNRcounter) = sum(abs([bits - bits_est]));

    %MMSE Equalizer
    hh_adjoint(1,1,:) = h_herm_h(2,2,:) + 10^(-SNR_dB(SNRcounter)/10);
    hh_adjoint(1,2,:) = -h_herm_h(1,2,:);
    hh_adjoint(2,1,:) = -h_herm_h(2,1,:);
    hh_adjoint(2,2,:) = h_herm_h(1,1,:) + 10^(-SNR_dB(SNRcounter)/10);

    hh_determinant = (hh_adjoint(1,1,:).*hh_adjoint(2,2,:) -
hh_adjoint(1,2,:).*hh_adjoint(2,1,:));
    hh_determinant = repmat(hh_determinant,[2,2,1]);

    hh_inverse = hh_adjoint./hh_determinant;

    hhy(1,1,:) = sum((h_conj_3d(:,1,:).*y_3d),1);
    hhy(2,1,:) = sum((h_conj_3d(:,2,:).*y_3d),1);

    hh_inverse_mul = hh_inverse;
    hh_inverse_mul(2,1,:) = hh_inverse(1,2,:);
    hh_inverse_mul(1,2,:) = hh_inverse(2,1,:);

    y_estimate(1,1,:) = sum((hh_inverse_mul(:,1,:).*hhy),1);
    y_estimate(2,1,:) = sum((hh_inverse_mul(:,2,:).*hhy),1);

    bits_estimate = real(y_estimate) > 0;

    bits_est = reshape(bits_estimate,[1,N]);

    err_MMSE(SNRcounter) = sum(abs([bits - bits_est]));

end

Calc_ber_ZF = err_ZF/N;
Calc_ber_MMSE = err_MMSE/N;
```

APPENDIX C

GENERATION OF ANTENNA PATTERN

```
clear all;

%=========================================================================
% Generation of Antenna pattern
% Aditya Kulkarni
% Ver. Date: 06/11/2014
%=========================================================================
% --------------------- PARAMETERS: ----------------------------------
% N = Number of Symbols for experiment
% SNR_dB = Signal-to-Noise Ratio in dB
% num_Tx = Number of transmit antennas
% num_Rx = Number of receive antennas
% a = maximum  swing in the antenna gain
% b = antenna gain offset
% phi = angular separation between the antennas
% l = Controls the rate of rotation of the aero-vehicle
%-------------------------------------------------------------------------

N = 1e6;

l = N/2;
pt = -(N/8):3*(N/8)-1;
phi = pi;
phi_arr = phi.*ones(1,l);

%Case 1: a/b = 1
a = 0.5;
b = 0.5;

%Relative antenna gain for a rotating body
sin_tx1 = b + a.*sin(2*pi*(1/l).*pt);

plot(linspace(-
pi,pi,length(sin_tx1)),10*log10(sin_tx1),'k','linewidth',2)
ylabel('Antenna gain (dB)','fontsize',14)
xlabel('Theta (rad)','fontsize',14)
axis([-4 4 -25 0])
set(gca,'fontsize',14)

%Case 2: a/b = 0.5
a = 0.25;

sin_tx1 = b + a.*sin(2*pi*(1/l).*pt);

figure()
plot(linspace(-
pi,pi,length(sin_tx1)),10*log10(sin_tx1),'k','linewidth',2)
ylabel('Antenna gain (dB)','fontsize',14)
xlabel('Theta (rad)','fontsize',14)
axis([-4 4 -25 0])
set(gca,'fontsize',14)

%Case 3: a/b = 0
a = 0;
```

```
sin_tx1 = b + a.*sin(2*pi*(1/l).*pt);

figure()
plot(linspace(-
pi,pi,length(sin_tx1)),10*log10(sin_tx1),'k','linewidth',2)
ylabel('Antenna gain (dB)','fontsize',14)
xlabel('Theta (rad)','fontsize',14)
axis([-4 4 -25 0])
set(gca,'fontsize',14)
```

APPENDIX D

THEORETICAL PLOTS

```
clear all;clc

%=========================================================================
====
% Theoretical output SNR for ZF and MMSE equalizers. This experiment
% studies the change in output SNR of the equalizers wrt SNR at the
% transmitter
% Ver. Date: 06/11/2014
%=========================================================================
====


N = 1e6;

SNR_dB = [0:2:40];
num_Rx = 2;
num_Tx = 2;
a = 0.5;
b = 0.5;


%Case 1: Stationary Rx and Tx
for SNRcounter = 1:length(SNR_dB)

   % Generate slow fading rayleigh coefficients
    h = 1/sqrt(2)*[randn(num_Tx,N) + 1j*randn(num_Tx,N)];

    % Model AWGN with 0dB variance
    n = 1/sqrt(2)*[randn(num_Tx,N/num_Tx) + 1j*randn(num_Tx,N/num_Tx)];

    % Receiver with ZF Equalization
    h_conj = conj(h);
    h_hermitian = h_conj;
    h_hermitian(2,1:2:end) = h_conj(1,2:2:end);
    h_hermitian(1,2:2:end) = h_conj(2,1:2:end);

    h_3d = reshape(h,[2,2,N/num_Tx]);
    h_conj_3d = reshape(h_conj,[2,2,N/num_Tx]);
    h_hermitian_3d = reshape(h_hermitian,[2,2,N/num_Tx]);

    h_herm_h(1,1,:) = sum(h_conj_3d(:,1,:).*h_3d(:,1,:),1);
    h_herm_h(1,2,:) = sum(h_conj_3d(:,1,:).*h_3d(:,2,:),1);
    h_herm_h(2,1,:) = sum(h_conj_3d(:,2,:).*h_3d(:,1,:),1);
    h_herm_h(2,2,:) = sum(h_conj_3d(:,2,:).*h_3d(:,2,:),1);

    hh_adjoint(1,1,:) = h_herm_h(2,2,:);
    hh_adjoint(1,2,:) = -h_herm_h(1,2,:);
    hh_adjoint(2,1,:) = -h_herm_h(2,1,:);
    hh_adjoint(2,2,:) = h_herm_h(1,1,:);

    hh_determinant = (hh_adjoint(1,1,:).*hh_adjoint(2,2,:) -
hh_adjoint(1,2,:).*hh_adjoint(2,1,:));
    hh_determinant = repmat(hh_determinant,[2,2,1]);
```

```
    hh_inverse = hh_adjoint./hh_determinant;


    rho_ZF1(SNRcounter) =
mean_nan((10^(.1*SNR_dB(SNRcounter))./(hh_inverse(1,1,:)));
    rho_ZF2(SNRcounter) =
mean_nan((10^(.1*SNR_dB(SNRcounter))./(hh_inverse(2,2,:)));

    rho_ZF_stationary = (rho_ZF1 + rho_ZF2)/2;

    hh_adjoint(1,1,:) = h_herm_h(2,2,:) + 10^(-SNR_dB(SNRcounter)/10);
    hh_adjoint(1,2,:) = -h_herm_h(1,2,:);
    hh_adjoint(2,1,:) = -h_herm_h(2,1,:);
    hh_adjoint(2,2,:) = h_herm_h(1,1,:) + 10^(-SNR_dB(SNRcounter)/10);

    hh_determinant = (hh_adjoint(1,1,:).*hh_adjoint(2,2,:) -
hh_adjoint(1,2,:).*hh_adjoint(2,1,:));
    hh_determinant = repmat(hh_determinant,[2,2,1]);

    hh_inverse1 = hh_adjoint./hh_determinant;

    rho_MMSE1(SNRcounter) =
mean_nan(((10^(.1*SNR_dB(SNRcounter))./hh_inverse1(1,1,:)) - 1);
    rho_MMSE2(SNRcounter) =
mean_nan((10^(.1*SNR_dB(SNRcounter))./(hh_inverse1(2,2,:)) - 1);

    rho_MMSE_stationary = (rho_MMSE1 + rho_MMSE2)/2;

end


%Case 2: Rotating Rx and Stationary Tx
for SNRcounter = 1:length(SNR_dB)

   % Generate slow fading rayleigh coefficients
    h = 1/sqrt(2)*[randn(num_Tx,N) + 1j*randn(num_Tx,N)];


    % Rotation of the aero-vehicle
    l = N/2;
    pt = 1:N/2;
    phi = pi;
    phi_arr = phi.*ones(1,l);

    sin_tx1 = b + a.*sin(2*pi*(100/l).*pt);
    sin_tx2 = b + a.*sin((2*pi*(100/l).*pt)+phi_arr);

    h(1,1:2:end) = h(1,1:2:end).*sin_tx1;
    h(1,2:2:end) = h(1,2:2:end).*sin_tx1;
    h(2,1:2:end) = h(2,1:2:end).*sin_tx2;
    h(2,2:2:end) = h(2,2:2:end).*sin_tx2;
```

```
    % Model AWGN with 0dB variance
    n = 1/sqrt(2)*[randn(num_Tx,N/num_Tx) + 1j*randn(num_Tx,N/num_Tx)];

    % Receiver with ZF Equalization
    h_conj = conj(h);
    h_hermitian = h_conj;
    h_hermitian(2,1:2:end) = h_conj(1,2:2:end);
    h_hermitian(1,2:2:end) = h_conj(2,1:2:end);

    h_3d = reshape(h,[2,2,N/num_Tx]);
    h_conj_3d = reshape(h_conj,[2,2,N/num_Tx]);
    h_hermitian_3d = reshape(h_hermitian,[2,2,N/num_Tx]);

    h_herm_h(1,1,:) = sum(h_conj_3d(:,1,:).*h_3d(:,1,:),1);
    h_herm_h(1,2,:) = sum(h_conj_3d(:,1,:).*h_3d(:,2,:),1);
    h_herm_h(2,1,:) = sum(h_conj_3d(:,2,:).*h_3d(:,1,:),1);
    h_herm_h(2,2,:) = sum(h_conj_3d(:,2,:).*h_3d(:,2,:),1);

    hh_adjoint(1,1,:) = h_herm_h(2,2,:);
    hh_adjoint(1,2,:) = -h_herm_h(1,2,:);
    hh_adjoint(2,1,:) = -h_herm_h(2,1,:);
    hh_adjoint(2,2,:) = h_herm_h(1,1,:);

    hh_determinant = (hh_adjoint(1,1,:).*hh_adjoint(2,2,:) -
hh_adjoint(1,2,:).*hh_adjoint(2,1,:));
    hh_determinant = repmat(hh_determinant,[2,2,1]);

    hh_inverse = hh_adjoint./hh_determinant;


    rho_ZF1(SNRcounter) =
mean_nan((10^(.1*SNR_dB(SNRcounter))./(hh_inverse(1,1,:)));
    rho_ZF2(SNRcounter) =
mean_nan((10^(.1*SNR_dB(SNRcounter))./(hh_inverse(2,2,:)));

    rho_ZF_Rx = (rho_ZF1 + rho_ZF2)/2;

    hh_adjoint(1,1,:) = h_herm_h(2,2,:) + 10^(-SNR_dB(SNRcounter)/10);
    hh_adjoint(1,2,:) = -h_herm_h(1,2,:);
    hh_adjoint(2,1,:) = -h_herm_h(2,1,:);
    hh_adjoint(2,2,:) = h_herm_h(1,1,:) + 10^(-SNR_dB(SNRcounter)/10);

    hh_determinant = (hh_adjoint(1,1,:).*hh_adjoint(2,2,:) -
hh_adjoint(1,2,:).*hh_adjoint(2,1,:));
    hh_determinant = repmat(hh_determinant,[2,2,1]);

    hh_inverse1 = hh_adjoint./hh_determinant;

    rho_MMSE1(SNRcounter) =
mean_nan(((10^(.1*SNR_dB(SNRcounter)))./hh_inverse1(1,1,:)) - 1);
    rho_MMSE2(SNRcounter) =
mean_nan((10^(.1*SNR_dB(SNRcounter)))./(hh_inverse1(2,2,:)) - 1);

    rho_MMSE_Rx = (rho_MMSE1 + rho_MMSE2)/2;
```

```
end



%Case 3: Rotating Tx and stationary Rx
for SNRcounter = 1:length(SNR_dB)

   % Generate slow fading rayleigh coefficients
    h = 1/sqrt(2)*[randn(num_Tx,N) + 1j*randn(num_Tx,N)];


    % Rotation of the aero-vehicle
    l = N/2;
    pt = 1:N/2;
    phi = pi;
    phi_arr = phi.*ones(1,l);

    sin_tx1 = b + a.*sin(2*pi*(100/l).*pt);
    sin_tx2 = b + a.*sin((2*pi*(100/l).*pt)+phi_arr);

    h(1,1:2:end) = h(1,1:2:end).*sin_tx1;
    h(1,2:2:end) = h(1,2:2:end).*sin_tx2;
    h(2,1:2:end) = h(2,1:2:end).*sin_tx1;
    h(2,2:2:end) = h(2,2:2:end).*sin_tx2;


    % Model AWGN with 0dB variance
    n = 1/sqrt(2)*[randn(num_Tx,N/num_Tx) + 1j*randn(num_Tx,N/num_Tx)];

    % Receiver with ZF Equalization
    h_conj = conj(h);
    h_hermitian = h_conj;
    h_hermitian(2,1:2:end) = h_conj(1,2:2:end);
    h_hermitian(1,2:2:end) = h_conj(2,1:2:end);

    h_3d = reshape(h,[2,2,N/num_Tx]);
    h_conj_3d = reshape(h_conj,[2,2,N/num_Tx]);
    h_hermitian_3d = reshape(h_hermitian,[2,2,N/num_Tx]);

    h_herm_h(1,1,:) = sum(h_conj_3d(:,1,:).*h_3d(:,1,:),1);
    h_herm_h(1,2,:) = sum(h_conj_3d(:,1,:).*h_3d(:,2,:),1);
    h_herm_h(2,1,:) = sum(h_conj_3d(:,2,:).*h_3d(:,1,:),1);
    h_herm_h(2,2,:) = sum(h_conj_3d(:,2,:).*h_3d(:,2,:),1);

    hh_adjoint(1,1,:) = h_herm_h(2,2,:);
    hh_adjoint(1,2,:) = -h_herm_h(1,2,:);
    hh_adjoint(2,1,:) = -h_herm_h(2,1,:);
    hh_adjoint(2,2,:) = h_herm_h(1,1,:);

    hh_determinant = (hh_adjoint(1,1,:).*hh_adjoint(2,2,:) -
hh_adjoint(1,2,:).*hh_adjoint(2,1,:));
```

```
    hh_determinant = repmat(hh_determinant,[2,2,1]);

    hh_inverse = hh_adjoint./hh_determinant;


    rho_ZF1(SNRcounter) =
mean_nan((10^(.1*SNR_dB(SNRcounter))./(hh_inverse(1,1,:)));
    rho_ZF2(SNRcounter) =
mean_nan((10^(.1*SNR_dB(SNRcounter))./(hh_inverse(2,2,:)));

    rho_ZF_Tx = (rho_ZF1 + rho_ZF2)/2;

    hh_adjoint(1,1,:) = h_herm_h(2,2,:) + 10^(-SNR_dB(SNRcounter)/10);
    hh_adjoint(1,2,:) = -h_herm_h(1,2,:);
    hh_adjoint(2,1,:) = -h_herm_h(2,1,:);
    hh_adjoint(2,2,:) = h_herm_h(1,1,:) + 10^(-SNR_dB(SNRcounter)/10);

    hh_determinant = (hh_adjoint(1,1,:).*hh_adjoint(2,2,:) -
hh_adjoint(1,2,:).*hh_adjoint(2,1,:));
    hh_determinant = repmat(hh_determinant,[2,2,1]);

    hh_inverse1 = hh_adjoint./hh_determinant;

    rho_MMSE1(SNRcounter) =
mean_nan(((10^(.1*SNR_dB(SNRcounter))./hh_inverse1(1,1,:)) - 1);
    rho_MMSE2(SNRcounter) =
mean_nan((10^(.1*SNR_dB(SNRcounter))./(hh_inverse1(2,2,:)) - 1);

    rho_MMSE_Tx = (rho_MMSE1 + rho_MMSE2)/2;
end
```

APPENDIX E

DESIGN OPTIMIZATION

```
%=========================================================================
% Percentage gain in performance of MMSE in comparison with ZF
% Ver. Date: 06/11/2014
%=========================================================================


%In this program I have tried compare the performance of ML and MMSE

clear all;close all hidden;clc
N = 1e6;
SNR_dB = [0:2:30];
num_Rx = 2;
num_Tx = 2;
b = 0.5;
a = 0.5;


for SNRcounter = 1:length(SNR_dB)

    % Generate random binary data
    bits = rand(1,N)>0.5; % creates 0s and 1s with equal probability
    BPSK_symbols = 2*bits-1; % generate  BPSK symbols

    %grouping the symbols in accordance with Spatial Multiplexing
    %techinique
    seq = repmat(BPSK_symbols,[num_Tx 1]);

    % Generate slow fading rayleigh coefficients
    h = 1/sqrt(2)*[randn(num_Tx,N) + 1j*randn(num_Tx,N)];


    % Rotation of the aero-vehicle
    l = N/2;
    pt = 1:N/2;
    phi = pi;
    phi_arr = phi.*ones(1,l);

    sin_tx1 = b + a.*sin(2*pi*(100/l).*pt);
    sin_tx2 = b + a.*sin((2*pi*(100/l).*pt)+phi_arr);

    h(1,1:2:end) = h(1,1:2:end).*sin_tx1;
    h(1,2:2:end) = h(1,2:2:end).*sin_tx2;
    h(2,1:2:end) = h(2,1:2:end).*sin_tx1;
    h(2,2:2:end) = h(2,2:2:end).*sin_tx2;


    % Model AWGN with 0dB variance
    n = 1/sqrt(2)*[randn(num_Tx,N/num_Tx) + 1j*randn(num_Tx,N/num_Tx)];

    % Y = HX + N
    y_add = zeros(size(seq,1),size(seq,2));
    y_temp = h.*seq;
    y_add(:,1:2:end) = y_temp(:,2:2:end);
    y_add = y_add + y_temp;
```

```
    y = y_add(:,1:2:end);

    y = y + 10^(-SNR_dB(SNRcounter)/20)*n;

    % Receiver with ZF Equalization
    h_conj = conj(h);
    h_hermitian = h_conj;
    h_hermitian(2,1:2:end) = h_conj(1,2:2:end);
    h_hermitian(1,2:2:end) = h_conj(2,1:2:end);

    h_3d = reshape(h,[2,2,N/num_Tx]);
    h_conj_3d = reshape(h_conj,[2,2,N/num_Tx]);
    h_hermitian_3d = reshape(h_hermitian,[2,2,N/num_Tx]);
    y_3d = reshape(y,[2,1,N/num_Tx]);

    h_herm_h(1,1,:) = sum(h_conj_3d(:,1,:).*h_3d(:,1,:),1);
    h_herm_h(1,2,:) = sum(h_conj_3d(:,1,:).*h_3d(:,2,:),1);
    h_herm_h(2,1,:) = sum(h_conj_3d(:,2,:).*h_3d(:,1,:),1);
    h_herm_h(2,2,:) = sum(h_conj_3d(:,2,:).*h_3d(:,2,:),1);

    hh_adjoint(1,1,:) = h_herm_h(2,2,:);
    hh_adjoint(1,2,:) = -h_herm_h(1,2,:);
    hh_adjoint(2,1,:) = -h_herm_h(2,1,:);
    hh_adjoint(2,2,:) = h_herm_h(1,1,:);

    hh_determinant = (hh_adjoint(1,1,:).*hh_adjoint(2,2,:) -
hh_adjoint(1,2,:).*hh_adjoint(2,1,:));
    hh_determinant = repmat(hh_determinant,[2,2,1]);

    hh_inverse = hh_adjoint./hh_determinant;

    hhy(1,1,:) = sum((h_conj_3d(:,1,:).*y_3d),1);
    hhy(2,1,:) = sum((h_conj_3d(:,2,:).*y_3d),1);

    hh_inverse_mul = hh_inverse;
    hh_inverse_mul(2,1,:) = hh_inverse(1,2,:);
    hh_inverse_mul(1,2,:) = hh_inverse(2,1,:);

    y_estimate(1,1,:) = sum((hh_inverse_mul(:,1,:).*hhy),1);
    y_estimate(2,1,:) = sum((hh_inverse_mul(:,2,:).*hhy),1);

    bits_estimate = real(y_estimate) > 0;

    bits_est = reshape(bits_estimate,[1,N]);

    err_ZF(SNRcounter) = sum(abs([bits - bits_est]));

    %MMSE Equalizer
    hh_adjoint(1,1,:) = h_herm_h(2,2,:) + 10^(-SNR_dB(SNRcounter)/10);
    hh_adjoint(1,2,:) = -h_herm_h(1,2,:);
    hh_adjoint(2,1,:) = -h_herm_h(2,1,:);
    hh_adjoint(2,2,:) = h_herm_h(1,1,:) + 10^(-SNR_dB(SNRcounter)/10);
```

```
    hh_determinant = (hh_adjoint(1,1,:).*hh_adjoint(2,2,:) -
hh_adjoint(1,2,:).*hh_adjoint(2,1,:));
    hh_determinant = repmat(hh_determinant,[2,2,1]);

    hh_inverse = hh_adjoint./hh_determinant;

    hhy(1,1,:) = sum((h_conj_3d(:,1,:).*y_3d),1);
    hhy(2,1,:) = sum((h_conj_3d(:,2,:).*y_3d),1);

    hh_inverse_mul = hh_inverse;
    hh_inverse_mul(2,1,:) = hh_inverse(1,2,:);
    hh_inverse_mul(1,2,:) = hh_inverse(2,1,:);

    y_estimate(1,1,:) = sum((hh_inverse_mul(:,1,:).*hhy),1);
    y_estimate(2,1,:) = sum((hh_inverse_mul(:,2,:).*hhy),1);

    bits_estimate = real(y_estimate) > 0;

    bits_est = reshape(bits_estimate,[1,N]);

    err_MMSE(SNRcounter) = sum(abs([bits - bits_est]));

end

Calc_ber_ZF = err_ZF/N;
Calc_ber_MMSE = err_MMSE/N;

err_tx = ((Calc_ber_ZF(1,1:end)-
Calc_ber_MMSE(1,1:end))./Calc_ber_ZF(1,1:end))*100;




for SNRcounter = 1:length(SNR_dB)

    % Generate random binary data
    bits = rand(1,N)>0.5; % creates 0s and 1s with equal probability
    BPSK_symbols = 2*bits-1; % generate  BPSK symbols

    %grouping the symbols in accordance with Spatial Multiplexing
    %techinique
    seq = repmat(BPSK_symbols,[num_Tx 1]);

    % Generate slow fading rayleigh coefficients
    h = 1/sqrt(2)*[randn(num_Tx,N) + 1j*randn(num_Tx,N)];


    % Rotation of the aero-vehicle
    l = N/2;
    pt = 1:N/2;
    phi = pi;
    phi_arr = phi.*ones(1,l);
```

```
    sin_tx1 = b + a.*sin(2*pi*(100/l).*pt);
    sin_tx2 = b + a.*sin((2*pi*(100/l).*pt)+phi_arr);

    h(1,1:2:end) = h(1,1:2:end).*sin_tx1;
    h(1,2:2:end) = h(1,2:2:end).*sin_tx1;
    h(2,1:2:end) = h(2,1:2:end).*sin_tx2;
    h(2,2:2:end) = h(2,2:2:end).*sin_tx2;


    % Model AWGN with 0dB variance
    n = 1/sqrt(2)*[randn(num_Tx,N/num_Tx) + 1j*randn(num_Tx,N/num_Tx)];

    % Y = HX + N
    y_add = zeros(size(seq,1),size(seq,2));
    y_temp = h.*seq;
    y_add(:,1:2:end) = y_temp(:,2:2:end);
    y_add = y_add + y_temp;
    y = y_add(:,1:2:end);

    y = y + 10^(-SNR_dB(SNRcounter)/20)*n;

    % Receiver with ZF Equalization
    h_conj = conj(h);
    h_hermitian = h_conj;
    h_hermitian(2,1:2:end) = h_conj(1,2:2:end);
    h_hermitian(1,2:2:end) = h_conj(2,1:2:end);

    h_3d = reshape(h,[2,2,N/num_Tx]);
    h_conj_3d = reshape(h_conj,[2,2,N/num_Tx]);
    h_hermitian_3d = reshape(h_hermitian,[2,2,N/num_Tx]);
    y_3d = reshape(y,[2,1,N/num_Tx]);

    h_herm_h(1,1,:) = sum(h_conj_3d(:,1,:).*h_3d(:,1,:),1);
    h_herm_h(1,2,:) = sum(h_conj_3d(:,1,:).*h_3d(:,2,:),1);
    h_herm_h(2,1,:) = sum(h_conj_3d(:,2,:).*h_3d(:,1,:),1);
    h_herm_h(2,2,:) = sum(h_conj_3d(:,2,:).*h_3d(:,2,:),1);

    hh_adjoint(1,1,:) = h_herm_h(2,2,:);
    hh_adjoint(1,2,:) = -h_herm_h(1,2,:);
    hh_adjoint(2,1,:) = -h_herm_h(2,1,:);
    hh_adjoint(2,2,:) = h_herm_h(1,1,:);

    hh_determinant = (hh_adjoint(1,1,:).*hh_adjoint(2,2,:) -
hh_adjoint(1,2,:).*hh_adjoint(2,1,:));
    hh_determinant = repmat(hh_determinant,[2,2,1]);

    hh_inverse = hh_adjoint./hh_determinant;

    hhy(1,1,:) = sum((h_conj_3d(:,1,:).*y_3d),1);
    hhy(2,1,:) = sum((h_conj_3d(:,2,:).*y_3d),1);

    hh_inverse_mul = hh_inverse;
    hh_inverse_mul(2,1,:) = hh_inverse(1,2,:);
    hh_inverse_mul(1,2,:) = hh_inverse(2,1,:);
```

```
    y_estimate(1,1,:) = sum((hh_inverse_mul(:,1,:).*hhy),1);
    y_estimate(2,1,:) = sum((hh_inverse_mul(:,2,:).*hhy),1);

    bits_estimate = real(y_estimate) > 0;

    bits_est = reshape(bits_estimate,[1,N]);

    err_ZF(SNRcounter) = sum(abs([bits - bits_est]));

    %MMSE Equalizer
    hh_adjoint(1,1,:) = h_herm_h(2,2,:) + 10^(-SNR_dB(SNRcounter)/10);
    hh_adjoint(1,2,:) = -h_herm_h(1,2,:);
    hh_adjoint(2,1,:) = -h_herm_h(2,1,:);
    hh_adjoint(2,2,:) = h_herm_h(1,1,:) + 10^(-SNR_dB(SNRcounter)/10);

    hh_determinant = (hh_adjoint(1,1,:).*hh_adjoint(2,2,:) -
hh_adjoint(1,2,:).*hh_adjoint(2,1,:));
    hh_determinant = repmat(hh_determinant,[2,2,1]);

    hh_inverse = hh_adjoint./hh_determinant;

    hhy(1,1,:) = sum((h_conj_3d(:,1,:).*y_3d),1);
    hhy(2,1,:) = sum((h_conj_3d(:,2,:).*y_3d),1);

    hh_inverse_mul = hh_inverse;
    hh_inverse_mul(2,1,:) = hh_inverse(1,2,:);
    hh_inverse_mul(1,2,:) = hh_inverse(2,1,:);

    y_estimate(1,1,:) = sum((hh_inverse_mul(:,1,:).*hhy),1);
    y_estimate(2,1,:) = sum((hh_inverse_mul(:,2,:).*hhy),1);

    bits_estimate = real(y_estimate) > 0;

    bits_est = reshape(bits_estimate,[1,N]);

    err_MMSE(SNRcounter) = sum(abs([bits - bits_est]));

end

Calc_ber_ZF = err_ZF/N;
Calc_ber_MMSE = err_MMSE/N;

err_rx = ((Calc_ber_ZF(1,1:end)-
Calc_ber_MMSE(1,1:end))./Calc_ber_ZF(1,1:end))*100;



figure()
plot(SNR_dB(1:end),err_tx,'kp','LineWidth',2,'MarkerSize',10);
hold on;
plot(SNR_dB(1:end),err_rx,'k^','LineWidth',2,'MarkerSize',10);
hold on;
```

```
Interp_tx = fit( SNR_dB(1:end)', err_tx' ,  'poly3' );
plot( Interp_tx, SNR_dB(1:end)', err_tx' );
hold  on;
Interp_rx = fit( SNR_dB(1:end)', err_rx' ,  'poly3' );
plot( Interp_rx, SNR_dB(1:end)', err_rx' );
grid on;
hleg  = legend('Tx rotation', 'Rx rotation','Location','SouthWest');
set(hleg,'fontsize',14)
xlabel('Eb/No (dB)','fontsize',14);
ylabel('Performance gain (in percentage)','fontsize',14);
title('Performance gain','fontsize',14)
set(gca,'fontsize',14)
```

BIBLIOGRAPHY

[1] Mietzner. J., Schober. R., Lampe L., Gerstacker W.H., Hoeher P.A., "Multiple-antenna techniques for wireless communications - a comprehensive literature survey," IEEE Communications Surveys & Tutorials, Volume 11, Issue 2, pp: 87 - 105, 2009

[2] S. M. Alamouti, "A simple transmit diversity technique for wireless communications," IEEE Journal on Selected Areas Communication, vol. 16, no. 8, pp. 1451–1458, Oct. 1998

[3] W. H. Gerstacker, F. Obernosterer, R. Schober, A. T. Lehmann, A. Lampe, and P. Gunreben, "Equalization concepts for Alamouti's space-time block code," IEEE Transaction on Communication, vol. 52, no. 7, pp. 1178–1190, July 2004

[4] V. Tarokh, N. Seshadri, and A. R. Calderbank, "Space-time codes for high data rate wireless communication: Performance criterion and code construction," IEEE Transactions on Information Theory, vol. 44, no. 2, pp. 744–765, Mar. 1998

[5] D. G. Brennan, "Linear diversity combining techniques," Proc. IRE, vol. 47, pp. 1075–1102, June 1959, Reprint: Proceedings of the IEEE, vol. 91, no. 2, pp. 331-356, Feb. 2003

[6] L. Zheng and D. N. C. Tse, "Diversity and multiplexing: A fundamental tradeoff in multiple-antenna channels," IEEE Transaction on Information Theory, vol. 49, no. 5, pp. 1073–1096, May 2003

[7] E. Telatar, "Capacity of multi-antenna Gaussian channels," European Transaction on Telecommunication, vol. 10, no. 6, pp. 585–595, Nov./Dec. 1999

[8] G. J. Foschini and M. J. Gans, "On limits of wireless communications in a fading environment when using multiple antennas," Kluwer Wireless Personal Communication, vol. 6, pp. 311–335, Mar. 1998

[9] D. Gesbert, M. Shafi, D. Shiu, P. J. Smith, and A. Naguib, "From theory to practice: An overview of MIMO space-time coded wireless systems," IEEE Journal on Selected Areas of Communication., vol. 21, no. 3, pp. 281–302, Apr. 2003

[10] A. J. Paulraj, D. A. Gore, R. U. Nabar, and H. Boelcskei, "An overview of MIMO communications – A key to gigabit wireless," Proceedings of the IEEE, vol. 92, no. 2, pp. 198–218, Feb. 2004

[11] Gupta B. and Saini D.S., "BER performance improvement in MIMO systems using various equalization techniques," 2012 2nd IEEE International Conference on Parallel Distributed and Grid Computing (PDGC), pp. 190- 194, 2012

[12] Yi Jiang, Mahesh K. Varanasi and Jian Li, "Performance Analysis of ZF and MMSE Equalizers for MIMO Systems: An In-Depth Study of the High SNR Regime," IEEE Transactions on Information Theory, Volume 57, Issue 4, pp. 2008 – 2026, 2011

[13] Sammuel Jalali, "Wireless Channel Equalization in Digital Communication Systems," CGU Theses & Dissertations, Claremont Graduate University, 2012

[14] Sarkar, S., Rahman, M.S., "Bit error rate improvement for QPSK modulation technique in a MIMO rayleigh fading channel by maximum likelihood equalization," 2012 7th International Conference on Electrical & Computer Engineering (ICECE), pp. 169 – 173, 2012

[15] Sergey Loyka, "On the Relationship of Information Theory and Electromagnetism," IEEE 6th International Symposium on Electromagnetic Compatibility and Electromagnetic Ecology, pages: 100-104, 2005

[16] Chizhik, D., Holmdel, Rashid-Fanokhi, F., Ling, J. and Lozano, A., "Antenna separation and capacity of BLAST in correlated channels," 2000 IEEE-APS Conference on Antennas and Propagation for Wireless Communications, pp. 183 - 185, 2000

[17] Wolniansky P.W., Holmdel, Foschini G.J., Golden G. D.,Valenzuela, R., "V-BLAST: an architecture for realizing very high data rates over the rich-scattering wireless channel," URSI International Symposium on Signals, Systems, and Electronics, Pp: 295 - 300, 1998

[18] Symon Haykin and Michael Moher, *Communication Systems*, 5th ed. Wiley, John & Sons, 2009

[19] David Tse and Pramod Vishwanath, *Fundamentals of Wireless Communication*, Cambridge University press, May 26, 2005

[20] Rodger Ziemer and Roger Peterson, *Introduction to Digital Communication*, 2nd ed. Prentice Hall, August 19, 2000

[21] Gerard J. Foschini, "Layered Space-Time Architecture for Wireless Communication in a Fading Environment When Using Multi-Element Antennas," Bell Labs Technical Journal, pp 41 - 59, autumn 1996

[22] Stephen Grant, Jung-Fu Cheng, Leonid Krasny, Karl Molnar, and Y.-P. Eric Wang, "Per-Antenna-Rate-Control (PARC) in Frequency Selective Fading with SIC-GRAKE Receiver," IEEE 60th Vehicular Technology Conference, VTC2004-Fall, pp: 1458 - 1462 Vol. 2, Sept 2004

[23] S. Loyka and F. Gagnon, "Performance analysis of the V-BLAST algorithm: An analytical approach," IEEE Transaction on Wireless Communication, vol. 3, no. 4, pp. 1326–1337, July 2004

[24] H. Zhu, Z. Lei, and F. P. S. Chin, "An improved square-root algorithm for BLAST," IEEE Signal Processing Letter., vol. 11, no. 9, pp. 772–775, Sept. 2004

[25] N. Boubaker, K. B. Letaief, and R. D. Murch, "Performance of BLAST over frequency-selective wireless communication channels," IEEE Transaction on Communication, vol. 50, no. 2, pp. 196–199, Feb. 2002

[26] Y. Huang, J. Zhang, and P. M. Djuric, "Bayesian detection for BLAST," IEEE Transaction on Signal Processing, vol. 53, no. 3, pp. 1086–1096, Mar. 2005

[27] Akrum Elkhazin, Konstantinos (Kostas) N. Plataniotis, and Subbarayan Pasupathy, "Reduced-dimension MAP turbo-BLAST detection," IEEE Transactions on Communication, vol. 54, no. 1, pp. 108–118, Jan. 2006

[28] Andrea Goldsmith, *Wireless Communications*, Cambridge University Press (August 8, 2005)

[29] "Resources and analysis for electronics engineers", *[online]*, http://www.radio-electronics.com/info/propagation/em_waves/electromagnetic_waves.php, date accessed: 06/13/14

VITA

Aditya Kulkarni was born in Bangalore, India. He completed his Bachelor's in Electronics and Communication in May, 2012. He has been working towards his master's degree at Missouri University of Science and Technology, Rolla, USA since August, 2012. He received his Master's degree from the Missouri University of Science and Technology in August, 2014.